PHYSICS REPORTS (Review Section of Physics Letters) 121, No. 5 (1985) 263–315. North-Holland, Amsterdam

COSMIC STRINGS AND DOMAIN WALLS

Alexander VILENKIN

Physics Department, Tufts University, Medford, MA 02155, U.S.A.

Received October 1984

Contents:

Abstract:

Phase transitions in the early universe can give rise to macroscopic topological defects: vacuum domain walls, strings, walls bounded by strings, and monopoles connected by strings. This article reviews the formation, physical properties and the cosmological evolution of various defects. A particular attention is paid to strings and their cosmological consequences, including the string scenario of galaxy formation and possible observational effects of strings.

Single orders for this issue

PHYSICS REPORTS (Review Section of Physics Letters) 121, No. 5 (1985) 263–315.

Copies of this issue may be obtained at the price given below. All orders should be sent directly to the Publisher. Orders must be accompanied by check.

Single issue price Dfl. 34.00, postage included.

0 370-1573/85/$18.55

COSMIC STRINGS AND DOMAIN WALLS

Alexander VILENKIN

Physics Department, Tufts University, Medford, MA 02155, U.S.A.

NORTH-HOLLAND–AMSTERDAM

1. Introduction

1. Overview

Recent developments in cosmology and particle physics were marked by a close interaction between the two fields. The connecting link was provided by Kirzhnits [1] who suggested that spontaneously broken symmetries can be restored at sufficiently high temperatures. According to modern ideas, the elementary particle interactions are described by a grand unified theory (GUT) with a simple gauge group G which is a valid symmetry at the highest energies. As the energy is lowered, the model undergoes a series of spontaneous symmetry breakings:

$$G \to H \to \cdots \to SU(3) \times SU(2) \times U(1) \to SU(3) \times U(1)_{em} .$$

In the context of hot big bang cosmology this implies a sequence of phase transitions in the early universe, with critical temperatures related to the corresponding symmetry breaking scales [2].

Phase transitions in the early universe can give rise to topologically stable defects – vacuum domain walls, strings and monopoles [3]. Hybrid topological animals – walls bounded by strings [4–6] and monopoles connected by strings [7, 8] – can also be formed. The first classification of topological defects and a discussion of their evolution were given by Kibble in 1976 [3]. Since that time, a great deal has been learned about the evolution and cosmological consequences of various defects. The main conclusions can be summarized as follows. Topologically stable domain walls and monopoles are disastrous for cosmological models and should be avoided [9, 10]. The hybrid structures are harmless: they rapidly break into pieces and decay practically without trace. Strings, on the other hand, cause no harm, but can lead to very interesting cosmological consequences. In particular, they can generate density fluctuations sufficient to explain the galaxy formation [11–13] and can produce a number of distinctive and unique observational effects. For strings of grand unification scale ($\sim 10^{16}$ GeV) some of these effects will soon be within the reach of experimental capabilities.

This paper reviews the formation, evolution and cosmological consequences of macroscopic topological defects. (That is, of all defects excluding monopoles. We will be interested in monopoles only in the context of monopoles connected by strings.) The reader will notice that, compared to other defects, strings occupy a prominent position in this review. The reason is that, of all the defects, they are the most interesting and much better studied. The paper is organized as follows. The remainder of chapter 1 gives some basic facts concerning the hot cosmological model and the physics of phase transitions in the early universe. Various types of defects and the conditions for their existence are discussed in chapter 2. Chapter 3 deals with the dynamics of strings and walls, their gravitational fields and their interaction with particles. The formation and cosmological evolution of topological defects are reviewed in chapter 4. Finally, chapter 5 discusses the cosmological implications of strings: their possible role in galaxy formation, observational effects of strings, and the possibility that we live in a string-dominated universe. Most of the material in this review has been published elsewhere, but some of the results are new.

Throughout the paper I use the notations $m_p = 2.2 \times 10^{-5}$ g $= 1.2 \times 10^{19}$ GeV and $t_p = 5.3 \times 10^{-44}$ s for the Planck mass and time, respectively, and the system of units in which $\hbar = c = 1$. In these units $t_p = m_p^{-1}$ and the gravitational constant is $G = m_p^{-2}$.

2. Standard cosmological model

In the standard hot cosmological model it is assumed that the universe begins in the state of local thermal equilibrium† at a very high temperature and then cools in the course of the cosmological expansion. The universe is assumed to be homogeneous and isotropic; besides, at early times the universe is very nearly flat, and thus it is accurately described by the spatially flat Robertson–Walker metric

$$ds^2 = dt^2 - a^2(t)\,(dx^2 + dy^2 + dz^2)\,. \tag{2.1}$$

The expansion of the universe is governed by the evolution equation

$$(\dot{a}/a)^2 = \tfrac{8}{3}\pi G\rho \tag{2.2}$$

where ρ is the energy density. The energy conservation law can be written as

$$\frac{d}{dt}(\rho a^3) = -P\frac{d}{dt}(a^3)\,, \tag{2.3}$$

where P is the pressure. In a radiation-dominated universe,

$$\rho = \frac{\pi^2}{30}N(T)\,T^4 \tag{2.4}$$

where $N(T) = N_b(T) + \frac{7}{8}N_f(T)$, $N_b(T)$ and $N_f(T)$ are, respectively, the numbers of distinct helicity states for bosons and fermions whose masses are small compared to T.

As long as the expansion of the universe is adiabatic, the entropy is conserved, and we can write

$$\frac{d}{dt}(sa^3) = 0 \tag{2.5}$$

where

$$s = \frac{2\pi^2}{45}N(T)\,T^3 \tag{2.6}$$

is the entropy density. If T is not near any mass threshold, $N(T) = \text{const.}$ and $aT = \text{const.}$ Then eqs. (2.2) and (2.3) give

$$a(t) \propto t^{1/2}\,, \tag{2.7}$$

† The word "local" is important here. A system in complete equilibrium necessarily has thermal energy density fluctuations which are much greater than one can afford in the early universe (large-scale density fluctuations grow by gravitational instability). It is assumed, therefore, that at time t the equilibrium is established only on scales smaller than the horizon, $\ell < t$, and that the universe is much smoother than the thermal state on scales $\ell > t$.

$$\rho = 3/(32\pi G t^2)\,, \tag{2.8}$$

$$T = (45/16\pi^3 NG)^{1/4} t^{-1/2} = 0.55(NG)^{-1/4} t^{-1/2}\,. \tag{2.9}$$

The equation of state of the universe in the radiation-dominated era is $P = \rho/3$.

When the universe becomes matter-dominated, $P \sim 0$ and we have

$$\frac{\mathrm{d}}{\mathrm{d}t}(\rho a^3) = 0\,, \tag{2.10}$$

$$a(t) \propto t^{2/3}\,, \tag{2.11}$$

$$\rho = (6\pi G t^2)^{-1}\,. \tag{2.12}$$

The transition between the two regimes occurs at the time of equal matter and radiation densities, $t \sim t_{\mathrm{eq}}$. We shall estimate t_{eq} later in this section.

Two important parameters characterizing the present universe are the Hubble "constant", $H = \dot{a}/a$, and the density, ρ. It is customary to use dimensionless parameters, h and Ω:

$$h = H/100\ \mathrm{km\,s^{-1}\,Mpc^{-1}}\,, \tag{2.13}$$

$$\Omega = \rho/\rho_{\mathrm{c}}\,, \tag{2.14}$$

where $\rho_{\mathrm{c}} = 2\times 10^{-29} h^2\ \mathrm{g\,cm^{-3}}$ is the critical density. Closed, open and flat universes correspond to $\Omega > 1$, $\Omega < 1$ and $\Omega = 1$, respectively. The inflationary cosmological model [23] predicts that $\Omega = 1$ with very high accuracy. Then eq. (2.11) applies at all $t > t_{\mathrm{eq}}$, and the present age of the universe can be found as

$$t_{\mathrm{pres}} = \tfrac{2}{3} H^{-1} = 2\times 10^{17} h^{-1}\,\mathrm{s}\,. \tag{2.15}$$

The actual values of h and Ω are known only approximately:

$$0.5 \lesssim h \lesssim 1\,, \tag{2.16}$$

$$0.1 \lesssim \Omega \lesssim 1\,. \tag{2.17}$$

Nucleosynthesis considerations require that the density of baryons, ρ_{B}, cannot exceed $0.1\rho_{\mathrm{c}}$,

$$\Omega_{\mathrm{B}} \lesssim 0.1\,, \tag{2.18}$$

and thus, if Ω is close to 1, the universe must be dominated by particles other than baryons.

In discussing the recent evolution of the universe, it is convenient to use the redshift parameter, z, defined as

$$1 + z = a(t_{\mathrm{pres}})/a(t)\,. \tag{2.19}$$

For $\Omega = 1$, $(1+z) \propto t^{-2/3}$.

The present temperature of the photon gas is $T = 2.7°K$ and the corresponding energy density is $\rho_\gamma = 4.5 \times 10^{-34}\,\mathrm{g\,cm^{-3}}$. The total density of "radiation", including photons and N_ν species of massless neutrons is

$$\rho_r = (1 + 0.23\,N_\nu)\,\rho_\gamma\,. \tag{2.20}$$

At $t > t_{eq}$ the ratio ρ_r/ρ decreases like $(1+z)$, and thus the time of equal matter and radiation densities, t_{eq}, corresponds to the redshift (for $N_\nu = 3$)

$$1 + z_{eq} = 2 \times 10^4\,\Omega h^2\,. \tag{2.21}$$

The density of the universe at t_{eq} is $\rho_{eq} = 3.2 \times 10^{-16}\,(\Omega h^2)^4\,\mathrm{g\,cm^{-3}}$. The time t_{eq} can be approximately found from $\rho_{eq} \approx 3/32\pi G t_{eq}^2$. This gives

$$t_{eq} \sim 4 \times 10^{10} (\Omega h^2)^{-2}\,\mathrm{s}\,. \tag{2.22}$$

An important event in the history of the universe is the decoupling of matter and radiation, when protons and electrons combine to form hydrogen atoms. This happens at

$$z_{dec} \approx 1300\,, \qquad t_{dec} \approx 5 \times 10^{11}\,(\Omega h^2)^{-1/2}\,\mathrm{s}\,. \tag{2.23}$$

This concludes my brief review of the standard cosmological model. For a detailed discussion, the reader is referred to the standard texts [23, 24].

It has been emphasized by a number of people that the initial conditions assumed in the standard cosmological model are rather unnatural (see, e.g., refs. [23, 3]). The required homogeneity could not be established by causal processes, the approximate flatness of the present universe requires a severe fine-tuning of the balance between kinetic and potential energies at early times, and the interaction rates at energies $>10^{17}$ GeV are insufficient to establish thermal equilibrium. An attractive solution to most of these problems (and also to the problem of overabundance of superheavy monopoles [10]) is given by the inflationary universe scenario [23] proposed by Guth. During the inflationary phase the universe is dominated by the false vacuum energy density, $\rho_v = \text{const.}$, and eq. (2.2) gives $a(t) \propto \exp(Ht)$, where $H = (8\pi G \rho_v/3)^{1/2}$. As a result of this exponential expansion, regions initially within the causal horizon are blown up to sizes much greater than the present Hubble radius. The vacuum energy eventually thermalizes, and the following evolution is the same as in the standard model. Any topological defects produced before inflation are inflated away, and one should be interested only in the defects produced after or near the end of inflation. In the following sections we shall assume, unless otherwise indicated, that the phase transitions of interest are not of inflationary type.

3. Cosmological phase transitions

Consider a field theory with a symmetry group G and a Higgs field ϕ with a potential of self-interaction $V(\phi)$. For illustrative purposes, it will be sufficient to take G = U(1) and

$$V(\phi) = \tfrac{1}{2}\lambda(\phi^+\phi - \eta^2)^2\,, \tag{3.1}$$

where ϕ is a complex scalar field and $\lambda > 0$. The U(1) symmetry is the symmetry of phase transformations, $\phi \to e^{i\alpha}\phi$. The minima of the potential are at nonzero values of ϕ, and so the symmetry is spontaneously broken and ϕ acquires a vacuum expectation value (VEV),

$$\langle\phi\rangle = \eta\, e^{i\theta}. \tag{3.2}$$

The magnitude of $\langle\phi\rangle$ is fixed by the model, but the phase θ is arbitrary. We thus have a manifold, M, of degenerate vacuum states corresponding to different choices of θ. In our example, M is a circle in the complex ϕ plane ($|\phi| = \eta$).

At finite temperatures the effective potential for ϕ acquires additional, temperature-dependent terms. In the high-temperature limit,

$$V_T(\phi) = A\, T^2\, \phi^+\, \phi + V(\phi), \tag{3.3}$$

where the dimensionless constant A is a combination of the self-coupling λ and other couplings of the field ϕ (e.g. Yukawa couplings and gauge coupling) [2]. Here we shall assume that $A > 0$. (The case $A < 0$ is discussed at the end of section 9.) From eqs. (3.1) and (3.3) we see that the effective mass of the field ϕ at temperature T is

$$m^2(T) = AT^2 - \lambda\eta^2. \tag{3.4}$$

$m^2(T)$ is equal to zero at $T = T_c$, where

$$T_c = (\lambda/A)^{1/2}\,\eta. \tag{3.5}$$

Unless λ is very small, we have $T_c \sim \eta$. For $T > T_c$, $m^2(T)$ is positive, the minimum of $V(\phi)$ is at $\phi = 0$, and so the expectation value of ϕ vanishes and the symmetry is restored. T_c is the critical temperature of the phase transition from the symmetric to the broken-symmetry phase. In our example the transition is second-order (the symmetric state $\langle\phi\rangle$ becomes unstable at $T < T_c$). More complicated models can lead to first-order phase transitions, where the symmetric phase remains metastable at $T < T_c$ and the transition occurs through bubble nucleation.

The general case of symmetry breaking, G→H, can be analyzed in a similar manner [2, 3]. In the symbolic relation G→H, G is the original group and H is its unbroken subgroup. H includes all elements of G which leave the VEV $\langle\phi\rangle$ invariant. The manifold of the equivalent vacuum states, M, can then be identified with the quotient space, G/H.

In the cosmological context, as the universe cools through the critical temperature T_c, the Higgs field ϕ will tend to develop an expectation value $\langle\phi\rangle$ corresponding to some point in the manifold M of equivalent vacua. However, since all points in M are equivalent, the choice will depend on random fluctuations and will be different in different regions of space. One can introduce the correlation length, ξ, such that the "directions" of $\langle\phi\rangle$ are uncorrelated at points separated by a distance greater than ξ. [In the model (3.1) the "direction" of $\langle\phi\rangle$ is determined by the phase θ, and ξ is the length beyond which the phases of $\langle\phi\rangle$ are uncorrelated.]

Correlations in the field ϕ can be described by a thermal average

$$G(|\boldsymbol{x} - \boldsymbol{x}'|) = \langle\phi^+(\boldsymbol{x}, t)\,\phi(\boldsymbol{x}', t)\rangle. \tag{3.6}$$

For the model (3.1) at $T > T_c$ we can write

$$G(|\boldsymbol{x}-\boldsymbol{x}'|) = 2\int_0^\infty \exp\{i\boldsymbol{k}(\boldsymbol{x}-\boldsymbol{x}')\}\{\exp(\omega_k/T)-1\}^{-1}\frac{d^3k}{(2\pi)^3\omega_k} \tag{3.7}$$

where $\omega_k^2 = k^2 + m^2(T)$ and I have subtracted the vacuum contribution to G, which is of no interest to us. We shall assume that T is sufficiently close to T_c, so that $m(T) \ll T$. Then it is easily shown that for $|\boldsymbol{x}-\boldsymbol{x}'| \equiv r \ll T^{-1}$ we have $G(r) = T^2/6$ and for $r \gg T^{-1}$

$$G(r) = \frac{T}{2\pi r}\exp\{-m(T)\,r\}. \tag{3.8}$$

At $T \to T_c$, $m(T) \to 0$ and the correlations decay with distance like r^{-1} for $r > T_c^{-1}$. Thus, for a second-order phase transition, the correlation length is given by[†]

$$\xi \sim T_c^{-1}. \tag{3.9}$$

For a first-order phase transition which proceeds through bubble nucleation and coalescence, the correlation length can be greatly increased. However, in any event, ξ should satisfy the causality constraint: correlations cannot establish on scales greater than the causal horizon: $\xi \lesssim \ell_H$ [3]. ℓ_H is defined as the distance travelled by light during the lifetime of the universe:

$$\ell_H(t) = a(t)\int_0^t \frac{dt'}{a(t')}. \tag{3.10}$$

If the phase transition is not of inflationary type (that is, if the universe does not become dominated by the vacuum energy), ℓ_H is always $\sim t$, and we can write

$$\xi \lesssim t_c, \tag{3.11}$$

where t_c is the time at which the phase transaction is completed.

Much of the initial random variation of $\langle\phi\rangle$ will die out in the course of further evolution, since a uniform Higgs field is energetically preferred. However, in many cases, topologically stable defects will be left behind which cannot, for topological reasons, be eliminated by a continuous evolution. The types of possible defects are determined by the topology of the manifold, M, as first discussed by Kibble [3]. (See also ref. [25].)

[†] It is often said that the correlation length in second-order phase transitions diverges at $T = T_c$. The apparent discrepancy is resolved very simply: the definition of the correlation length used in condensed matter physics is different from our definition of ξ. A condensed matter physicist defines the correlation radius r_c as the distance beyond which correlations decay exponentially. In our example, $r_c \sim 1/m(T) \to \infty$ as $T \to T_c$.

2. Topological defects

4. Domain walls

Domain walls are formed when a discrete symmetry is broken. The simplest model of this sort is

$$L = \tfrac{1}{2}(\partial_\mu \phi)^2 - \tfrac{1}{2}\lambda(\phi^2 - \eta^2)^2 \tag{4.1}$$

where ϕ is a real scalar field. The symmetry is $Z_2: \phi \to -\phi$, the minima of $V(\phi)$ are at $\phi = \pm\eta$, and so the manifold M consists of only two points. As we go from a region with $\langle\phi\rangle = +\eta$ to a region with $\langle\phi\rangle = -\eta$, we should necessarily pass through $\langle\phi\rangle = 0$, and thus the two regions must be separated by a domain wall of false vacuum.

The wall is described by a classical solution of the field equation

$$\Box\phi + 2\lambda\phi(\phi^2 - \eta^2) = 0\,. \tag{4.2}$$

For a plain wall in the xy-plane the solution is [9]

$$\phi_0(z) = \eta \tanh(z/\delta)\,, \tag{4.3}$$

where $\delta = \lambda^{-1/2}\eta^{-1}$ is the thickness of the wall. The false vacuum energy density is $\rho_v \sim \lambda\eta^4$, and the surface energy density of the wall is $\sigma \sim \rho_v\delta \sim \lambda^{1/2}\eta^3$. To calculate σ exactly, we can compute the energy-momentum tensor for the solution (4.3),

$$T_{\mu\nu} = \partial_\mu\phi\,\partial_\nu\phi - g_{\mu\nu}L\,. \tag{4.4}$$

This gives

$$T^\nu_\mu = f(z)\,\mathrm{diag}(1, 1, 1, 0) \tag{4.5}$$

where

$$f(z) = \lambda\eta^4[\cosh(z/\delta)]^{-4} \tag{4.6}$$

is a bell-shaped function of width $\sim\delta$ peaked at $z = 0$. The surface energy density is given by

$$\sigma = \int T^0_0\,\mathrm{d}z = \tfrac{4}{3}\lambda^{1/2}\eta^3\,. \tag{4.7}$$

Note the important fact that T^ν_μ in eq. (4.5) is invariant with respect to Lorentz boosts in the xy-plane. This is not surprising, since $\phi_0(z)$ is a scalar field independent of x, y, t, and thus having the same invariance. Therefore, it makes sense to talk only about transverse motion of the wall; motion in tangential directions is unobservable. Strictly speaking, this applies only to plane walls, but macroscopic walls with curvature radii $R \gg \delta$ can locally be considered as flat.

In general, domain walls form when the manifold M has two or more disconnected pieces. They can

be classified by the homotopy group $\pi_0(M)$, which counts the disconnected components of M. [In our example $\pi_0(M) = Z_2$.] Examples of GUTs with domain walls can be found in ref. [8].

5. Strings

The simplest model that gives rise to strings is that of a complex scalar field ϕ with a self-interaction of the form (3.1). After the phase transition ϕ develops a VEV $\langle\phi\rangle = \eta\, e^{i\theta}$, where θ varies on the scale of the correlation length ξ. Since $\langle\phi\rangle$ is single valued, the total change of θ around any closed loop in space must be equal to $2\pi n$, where n is an integer:

$$\Delta\theta = 2\pi n\,. \tag{5.1}$$

Consider a closed loop with $\Delta\theta = 2\pi$ and imagine continuously shrinking the loop to a point. If no singularities are encountered, the value $n = 1$ in eq. (5.1) cannot discontinuously change to $n = 0$, and thus we must encounter at least one point where the phase θ is undefined (which means $\langle\phi\rangle = 0$). This shows that at least one tube of false vacuum should be caught inside any loop which has $\Delta\theta \neq 0$. It is clear that such tubes, which are called strings, can have no ends and must be infinite or closed (otherwise, it would be possible to contract the loop without crossing the string).

The properties of strings produced by breaking local and global symmetries are somewhat different. First consider the case of a local U(1) symmetry,

$$L = D_\mu\phi^+ D^\mu\phi - \tfrac{1}{4}F_{\mu\nu}F^{\mu\nu} - \tfrac{1}{2}\lambda(\phi^+\phi - \eta^2)^2\,, \tag{5.2}$$

where $D_\mu = \partial_\mu - igA_\mu$, $F_{\mu\nu} = \partial_\mu A_\nu - \partial_\nu A_\mu$ and g is the gauge coupling. A string solution in this model was first discussed by Nielsen and Olesen [26]. In cylindrical coordinates (r, θ, z) the Higgs field at large distances from the string has the form

$$\phi \approx \eta\, e^{in\theta}\,, \tag{5.3}$$

where n is an integer, and the gauge field is

$$A_\mu \approx \frac{1}{ig}\partial_\mu \ln\phi\,. \tag{5.4}$$

The asymptotic forms (5.3) and (5.4) are such that $F_{\mu\nu} = 0$ and $D_\mu\phi = 0$, so that the energy density vanishes outside the string core. (These forms are approached exponentially as $r \to \infty$ [26].) Using the Stokes' theorem we find

$$\int \boldsymbol{B}\cdot d\boldsymbol{S} = \oint \boldsymbol{A}\cdot d\boldsymbol{\ell} = 2\pi n/g\,, \tag{5.5}$$

where $\boldsymbol{B} = \nabla \times \boldsymbol{A}$ is the magnetic gauge field. We see that the string carries n units of elementary magnetic flux. [Strings in this model are very similar to the quantized tubes of magnetic flux in superconductors.] An elementary string corresponds to $n = \pm 1$. Strings with $|n| > 2$ are probably unstable and decay into elementary ones [42].

The radius of the string core is determined by the Compton wavelengths of the Higgs and vector mesons: $\delta_\phi \sim m_\phi^{-1}$ and $\delta_A \sim m_A^{-1}$, where $m_\phi = \lambda^{1/2}\eta$ and $m_A = g\eta$ are the corresponding masses. For $m_\phi < m_A$, which is usually the case, the string has an inner core of false vacuum with linear mass density $\mu_\phi \sim \rho_v \delta_\phi^2 \sim \eta^2$, and a tube of magnetic field of radius $\delta_A > \delta_\phi$ with $\mu_A \sim B^2\delta^2 \sim \eta^2$. Thus, the total mass of string per unit length is [26, 3]

$$\mu \sim \eta^2 . \tag{5.6}$$

Strings of cosmological interest have sizes much greater than their width. In this case the internal structure of the string is unimportant and physical quantities of interest, such as the energy-momentum tensor T^ν_μ, can be averaged over the cross-section. For a static straight string lying along the z-axis we define

$$\tilde{T}^\nu_\mu = \delta(x)\,\delta(y)\int T^\nu_\mu \,\mathrm{d}x\,\mathrm{d}y . \tag{5.7}$$

The string solution is invariant under Lorentz boosts in the z-direction, and thus $\tilde{T}^0_0 = \tilde{T}^3_3$ with all other components equal to zero except, perhaps, $\tilde{T}^i_j$ with $i = 1, 2$. To show that these remaining components are also equal to zero, we can use the conservation law, $T^i_{i,j} = 0$, and write

$$\int T^i_{i,j}\, x^k \,\mathrm{d}x\,\mathrm{d}y = 0 , \tag{5.8}$$

where all indices take values 1 or 2. Integration by parts gives

$$\int T^k_i \,\mathrm{d}x\,\mathrm{d}y = 0 \qquad (i, k = 1, 2) . \tag{5.9}$$

Thus, the energy-momentum tensor of the string is given by

$$\tilde{T}^\nu_\mu = \mu\ \mathrm{diag}(1, 0, 0, 1)\,\delta(x)\,\delta(y) . \tag{5.10}$$

The tension along the string is equal to the energy density. [One can say that the general form of $T_{\mu\nu}$ for walls and strings can be obtained from the vacuum energy-momentum tensor by dimensional reduction. In vacuum, Lorentz invariance requires that $T^\nu_\mu \propto g^\nu_\mu = \mathrm{diag}(1, 1, 1, 1)$.]

6. *More complicated strings*

Breaking a U(1) symmetry is one but not the only way to make strings. In the general case, strings are formed when the manifold M of equivalent vacua is not simply connected (that is, if it contains unshrinkable loops). Strings are classified by the first homotopy group π_1 (M), which counts the equivalence classes of loops in M. In the example of the previous section G = U(1), M is a circle and $\pi_1(\mathrm{M}) = \mathrm{Z}$, the group of integers (they are the integers appearing in eqs. (5.1) and (5.5)). The general condition for the formation of strings can thus be written as

$$\pi_1(\mathrm{M}) \neq \mathrm{I} , \tag{6.1}$$

where I is the trivial group.

The following theorem from the homotopy theory is very useful for analyzing the topological defects. Suppose that the group G is broken to a subgroup H: $G \to H$.

Theorem. If $\pi_n(G) = \pi_{n-1}(G) = I$, then

$$\pi_n(M) = \pi_{n-1}(H), \tag{6.2}$$

where the equality sign "=" indicated isomorphism.

In particular, if $\pi_1(G) = \pi_0(G) = I$, then

$$\pi_1(M) = \pi_0(H). \tag{6.3}$$

Equations (6.1), (6.3) imply that strings can be formed in a phase transition $G \to H$ only if $\pi_0(H) \neq I$. This means that the unbroken group H should contain a discrete symmetry [27]. (This conclusion does not apply to the model (5.2), since $\pi_1[U(1)] = Z \neq I$.) A fairly common example of this sort is when the group H is a product of a continuous group and Z_2, e.g. [27]

$$SO(10) \to SU(5) \times Z_2. \tag{6.4}$$

Z_2 strings formed in this phase transition have no direction and any two parallel strings can be annihilated by one another. Examples of realistic GUTs with strings can be found in refs. [13, 27, 28].

If the symmetry breaking is $G \to K \times Z_n$ with $n > 3$, then strings can form vertices with several strings joining at the vertex. Even more exotic strings are formed when the first homotopy group $\pi_1(M)$ is non-Abelian. In this case the strings corresponding to noncommuting elements of $\pi_1(M)$ cannot pass through one another [29, 3] (More exactly, when two such strings move through one another, a third string is formed stretching between the two.) No realistic models with noncommuting strings have yet been suggested.

7. *Global strings*

Strings can be formed as a result of local as well as global symmetry breakings. We shall call them local and global strings, respectively. The topological conditions for the formation of strings are the same in both cases, but the physical properties of local and global strings are somewhat different. Local strings were discussed in section 5, and here we shall concentrate on global strings [5].

The simplest case is that of a global U(1) symmetry. The Lagrangian is given by eq. (5.2) with A_μ set equal to zero:

$$L = \partial_\mu \phi^+ \partial^\mu \phi - \tfrac{1}{2}\lambda(\phi^+\phi - \eta^2)^2. \tag{7.1}$$

Like before, the phase of ϕ changes by 2π around the string, the radius of the core is $\delta \sim \lambda^{-1/2}\eta^{-1}$, and outside the core ϕ is given by $\phi = \eta \exp(i\theta)$. But now there is no gauge field to compensate the variation of the phase θ at $r \gg \delta$ (and, of course, there is no magnetic flux associated with the string). The mass per unit length of the string is

$$\mu \sim \eta^2 + \int_{\delta}^{R} \left| \frac{1}{r} \frac{\partial \phi}{\partial \theta} \right|^2 2\pi r \, dr \approx 2\pi\eta^2 \ln \frac{R}{\delta}, \tag{7.2}$$

where R is the cut-off radius. We see that μ logarithmically diverges as $R \to \infty$. Note, however, that the energy of a closed loop is always finite: $E \sim \eta^2 R \ln(R/\delta)$, where R is the size of the loop and I have assumed that the loop is momentarily at rest. The $\ln R$ factor reflects a long-range interaction between different parts of the loop, which is due to the presence of a massless Goldstone boson. Two parallel strings with opposite signs of $\Delta\theta$ attract one another with a force per unit length $F \sim \eta^2/R$, where R is the distance between the strings. (Compare with local strings for which the interaction dies out exponentially with distance.) Note also that global strings are analogous to quantized vortex lines in liquid helium.

Realistic grand unified models with global strings can be easily constructed [5, 30]. The simplest model is the minimal SU(5) which has an "accidental" global B − L U(1) symmetry. Breaking $U(1)_{B-L}$ gives rise to strings.

8. *Monopoles*

Monopoles [31] are point defects which form when the manifold of equivalent vacua, M, contains unshrinkable surfaces, that is, when

$$\pi_2(M) \neq I. \tag{8.1}$$

$\pi_2(M)$ is the homotopy group classifying unshrinkable surfaces in M.

Suppose that the group G is such that $\pi_1(G) = \pi_2(G) = I$ (all currently popular grand unified groups satisfy this condition). Then, applying the Theorem of section 6 for $n = 2$ we find

$$\pi_2(M) = \pi_1(H). \tag{8.2}$$

From (8.1) and (8.2) we obtain the condition for the formation of monopoles: $\pi_1(H) \neq I$. For example, monopoles will be formed at a phase transition

$$G \to K \times U(1) \tag{8.3}$$

(since $\pi_1[U(1)] = Z$). In the sequence of symmetry breakings from G down to $SU(3) \times U(1)_{em}$, a U(1) factor must first appear at some stage, and thus the formation of monopoles in the early universe cannot be avoided.

For monopoles produced as a result of a local symmetry breaking, the energy density decays exponentially with distance form the center. The mass of such monopoles is [3]

$$m \sim 4\pi\eta/g. \tag{8.4}$$

For global monopoles, the variation of the Higgs field ϕ outside the core is not compensated by a gauge

field, and the total energy is linearly divergent. This means that monopoles and antimonopoles are attracted with a confining force independent of the distance.

In this paper we will be interested in monopoles only in the context of monopoles connected by strings (see the next section). For a detailed discussion of monopoles and their evolution, see refs. [3, 10] and Preskill's paper in ref. [23].

9. *Monopoles connected by strings*

Monopoles formed at a phase transition can get connected to strings at a subsequent phase transition [7, 8]. A typical sequence of phase transitions leading to this series of events is

$$G \to K \times U(1) \to K . \tag{9.1}$$

The first phase transition gives monopoles carrying the magnetic flux of the U(1) gauge field. At the second transition the magnetic field is squeezed into flux tubes connecting monopoles and antimonopoles. Closed and infinite strings can also be formed.

In this class of models strings are not topologically stable and can break producing monopoles and antimonopoles at the free ends. However, breaking of the string is a tunneling process and its probability is typically very small. A semiclassical calculation gives [7]

$$p \propto \exp(-\pi m^2/\mu) , \tag{9.2}$$

where m is the monopole mass and μ is the string tension.

An interesting model of the type (9.1) has been suggested by Langacker and Pi [32] as a possible solution to the problem of overabundance of superheavy monopoles. The sequence of phase transitions is

$$SU(5) \to SU(3) \times SU(2) \times U(1) \to SU(3) \to SU(3) \times U(1)_{em} . \tag{9.3}$$

Monopoles formed at the first transition get connected by strings at the second phase transition. But at the third phase transition the U(1) symmetry is restored and the strings disappear.

The possibility of a symmetry *restoration* at low temperatures was first discussed by Weinberg [2]. The properties of topological defects in this type of models are somewhat different from the usual case, and we shall briefly discuss the difference. Consider a finite-temperature effective potential of the form

$$V_T(\phi) = m^2(T)\, \phi^+ \phi + \tfrac{1}{2}\lambda\, (\phi^+ \phi)^2 , \tag{9.4}$$

where

$$m^2(T) = m^2(0) + AT^2 . \tag{9.5}$$

The parameter A is determined by the interaction of ϕ with effectively massless degrees of freedom. A can be approximately constant over a wide range of temperatures, but can also change at mass thresholds and at phase transitions. It is usually assumed that $m^2(0) < 0$ and $A > 0$. Then the symmetry is broken at low temperatures and the analysis of section 3 applies. Suppose now that $m^2(0) > 0$ and that

A becomes negative below some temperature $T_1 \gg m(0)$. Then at $T < T_1$ the symmetry is broken and ϕ develops a VEV

$$|\langle\phi\rangle| = (|A|/\lambda)^{1/2}\, T(1 - T_2^2/T^2)^{1/2}\,, \tag{9.6}$$

where $T_2 = |A|^{-1/2}\, m(0) \ll T_1$. At $T = T_2$, $\langle\phi\rangle = 0$, and below T_2 the symmetry is restored. (Quasi) stable string solutions exist only in the range $T_1 > T > T_2$. For $T \gg T_2$, the width of the strings is $\delta \sim 1/|m(T)| \sim |A|^{-1/2} T^{-1}$, the false "vacuum" energy density is $\rho_v \sim \lambda\langle\phi\rangle^4 \sim A^2\lambda^{-1}T^4$, and the linear mass density of the string is

$$\mu \sim (|A|/\lambda)T^2\,. \tag{9.7}$$

As $T \to T_2$, we have $\delta \to \infty$, $\mu \to 0$, and the strings "dissolve". The most important difference of this model from the usual case is that the physical characteristics of strings depend on the temperature in an essential way.

10. Walls bounded by strings

Consider the sequence of symmetry breakings

$$G \to K \times Z_2 \to K\,. \tag{10.1}$$

The first transition gives rise to strings (see section 6) which get connected by domain walls at the second phase transition [4, 6].

Walls bounded by strings can also be formed due to breaking of an approximate symmetry [5]. As an example consider a model with an approximate global U(1) symmetry

$$L = \partial_\mu\phi^+\partial^\mu\phi - \tfrac{1}{2}\lambda(\phi^+\phi - \eta^2)^2 + 2m^4(\cos N\theta - 1)\,, \tag{10.2}$$

where θ is the phase of ϕ, $\phi = \rho\, e^{i\theta}$, and N is an integer. This is a reduced version of the invisible axion models designed to solve the strong CP problem [33–35]. In such models $m \sim 1$ GeV and $\eta \gg m$ (typically, $\eta \sim 10^9$–10^{12} GeV). The approximate U(1) symmetry of (10.2) corresponds to the anomalous chiral Peccei–Quinn symmetry which is explicitly broken by instantons at the strong interaction mass scale m. We shall first consider the case of $N = 1$, when the potential has the shape of a Mexican hat slightly tilted by the presence of the θ-dependent term.

The field ϕ acquires a nonzero VEV when the universe cools to a temperature $T \sim \eta$. At such temperatures the last term in (10.2) is negligible, and we get global U(1) strings, as discussed in section 8. At sufficiently low temperatures the θ-dependent term in (10.2) becomes important. The minimum of energy (for $N = 1$) corresponds to $\theta = 0 \pmod{2\pi}$. However, the phase θ cannot become equal to zero everywhere, since it changes by $\Delta\theta = 2\pi$ around the strings. Hence, θ tends to settle down to zero at all points around a string, except within a domain wall, so that θ changes by 2π across the wall [5].

To see that the model (10.2) indeed has domain wall solutions, we note that, away from the string cores, the VEV of ϕ is $\langle\phi\rangle = \eta\, e^{i\theta}$, and the effective Lagrangian for θ is

$$L_\theta = \eta^2\, \partial_\mu\theta\, \partial^\mu\theta + 2m^4(\cos\theta - 1)\,. \tag{10.3}$$

The corresponding wave equation is

$$\Box\theta + m_a^2 \sin\theta = 0\,, \tag{10.4}$$

where $m_a = m^2/\eta$ is the axion mass. Equation (10.4) is the so-called sine-Gordon equation which is known to have domain wall solutions (solitons) [25]:

$$\theta(x) = 4\tan^{-1}\exp(m_a x)\,, \tag{10.5}$$

where x is the axis perpendicular to the wall. The thickness of the wall is $\delta \sim m_a^{-1}$ and the energy per unit area is [25]

$$\sigma = 16m^2\eta\,. \tag{10.6}$$

Domain walls in this model (as well as in the model (10.1)) are not topologically stable, and there is a nonzero probability for the formation of a hole in the wall bounded by a string. However, for $m < \eta$ the tunneling probability is exponentially small [4].

The analysis of the case $N \geq 2$ is very similar, and here I shall only indicate the differences. The minima of the potential are at $\theta = 2\pi n/N$ with $n = 0, 1, \ldots, N-1$, and so there are N distinct vacua which can be separated by topologically stable walls [34]. The phase θ changes by $2\pi/N$ across the "minimal" wall. (There can be walls with $\Delta\theta = 2\pi n/N$, but they are probably unstable.) Since θ changes by 2π around a string, each string gets N domain walls attached to it.

3. Physical processes with strings and walls

11. Dynamics of strings

In this section we shall discuss the dynamics of macroscopic strings assuming that their dimensions are much greater than the thickness δ.

The space–time trajectory of a string can be parametrized as

$$x^\mu = x^\mu(\zeta^a)\,; \qquad a = 0, 1 \tag{11.1}$$

where ζ^0 is a timelike and ζ^1 is a spacelike parameter. In this and most of the following sections we shall consider only local strings which do not interact with a long-range Goldstone field. The action functional, S, for such strings should satisfy the following requirements: (i) S should be invariant under general coordinate transformations; (ii) S should be invariant with respect to a reparametrization

$$\zeta^a \to \tilde{\zeta}^a(\zeta)\,; \tag{11.2}$$

(iii) the action should have the form of an integral over the 2-dimensional world sheet (11.1). The "building blocks" for the action are the functions $x^\mu(\zeta^a)$ and the string tension, μ.

These three conditions determine the action uniquely, up to a numerical factor:

$$S = -\mu \int [-g^{(2)}]^{1/2} \, d^2\zeta, \tag{11.3}$$

where $g^{(2)}$ is the determinant of the 2-dimensional metric tensor on the surface, $g^{(2)}_{ab} = g_{\mu\nu} x^{\mu}_{,a} x^{\nu}_{,b}$ and $x^{\mu}_{,a} = \partial x^{\mu}/\partial \zeta^a$:

$$g^{(2)} = \dot{x}^2 x'^2 - (\dot{x} \cdot x')^2 . \tag{11.4}$$

Here, $a \cdot b = a^{\mu} b_{\mu}$, $\dot{x}^{\mu} = \partial x^{\mu}/\partial \zeta^0$ and $x'^{\mu} = \partial x^{\mu}/\partial \zeta^1$.

Equation (11.3) is the Nambu action for a relativistic string [26, 36]; the integral in this equation is just the surface area of the world sheet described by the string. If we take ζ^1 to be the length along the string ℓ and ζ^0 to be the time t, then eq. (11.3) takes the form [26]

$$S = -\mu \int dt \int d\ell \, (1 - v_{\perp}^2)^{1/2}, \tag{11.5}$$

where

$$\boldsymbol{v}_{\perp} = \frac{\partial \boldsymbol{x}}{\partial t} - \frac{\partial \boldsymbol{x}}{\partial \ell} \left(\frac{\partial \boldsymbol{x}}{\partial t} \cdot \frac{\partial \boldsymbol{x}}{\partial \ell} \right) \tag{11.6}$$

is the transverse velocity. Equation (11.5) is easily understood if we note that only the transverse motion of the string is physically observable.

The equations of motion for a string are

$$\frac{\partial}{\partial \zeta^a} \left(\frac{\partial L}{\partial x^{\mu}_{,a}} \right) - \frac{\partial L}{\partial x^{\mu}} = 0 \tag{11.7}$$

where $L = -\mu [-g^{(2)}]^{1/2}$ is the string Lagrangian. The last term in (11.7) is nonzero only if the metric $g_{\mu\nu}$ depends on x^{μ}. Let us first consider the dynamics of strings in flat space–time, where eq. (11.7) takes the form

$$\frac{\partial}{\partial \zeta^0} \left\{ \frac{(\dot{x} \cdot x') \, x'^{\mu} - x'^2 \dot{x}^{\mu}}{[(\dot{x} \cdot x')^2 - \dot{x}^2 x'^2]^{1/2}} \right\} + \frac{\partial}{\partial \zeta^1} \left\{ \frac{(\dot{x} \cdot x') \, \dot{x}^{\mu} - \dot{x}^2 x'^{\mu}}{[(\dot{x} \cdot x')^2 - \dot{x}^2 x'^2]^{1/2}} \right\} = 0 . \tag{11.8}$$

The equations of motion can be simplified by a suitable choice of the parameters ζ^0, ζ^1. We can choose ζ^0 to be the time coordinate and ζ^1 to be one of the spatial coordinates, say,

$$\zeta^0 = t, \qquad \zeta^1 = x . \tag{11.9}$$

Then the string trajectory is described by two functions, $y(x, t)$ and $z(x, t)$, and it is easily verified that

$$y = f(x \pm t), \qquad z = g(x \pm t) \tag{11.10}$$

is a solution of eq. (11.8) for arbitrary functions f and g [38]. These solutions describe waves of arbitrary

shape propagating along the string with the velocity of light. Note that a superposition of waves travelling in opposite directions is not, in general, a solution, since eq. (11.8) is nonlinear.

A different choice of parameters ζ^0, ζ^1 is convenient for studying closed loops of strings. The gauge freedom (11.2) allows us to impose two gauge conditions which we can choose as [36, 37]

$$\dot{x}\cdot x' = 0\,; \qquad \dot{x}^2 + x'^2 = 0\,. \tag{11.11}$$

(x'^μ and $\dot{x}^\mu$ are spacelike and timelike, respectively.) Then the equation of motion (11.8) takes the form of a wave equation

$$\ddot{x}^\mu + x''^\mu = 0\,. \tag{11.12}$$

The conditions (11.11) do not fix the gauge completely. There still remains the freedom of transformations (11.2) with $\dot{\tilde{\zeta}}^1 = \tilde{\zeta}^{0\prime}$, $\tilde{\zeta}^{1\prime} = \dot{\tilde{\zeta}}^0$, which implies

$$\ddot{\tilde{\zeta}}^a - \tilde{\zeta}^{a\prime\prime} = 0\,. \tag{11.13}$$

We can use this remaining freedom to set $\tilde{\zeta}^0 = x^0$ [note that this is consistent with eqs. (11.12), (11.13)]. Then the trajectory of the string is described by a vector function $\boldsymbol{x}(\zeta, t)$, where I have set $\zeta^1 \equiv \zeta$, and eqs. (11.11), (11.12) give

$$\dot{\boldsymbol{x}}\cdot\boldsymbol{x}' = 0\,; \qquad \dot{\boldsymbol{x}}^2 + \boldsymbol{x}'^2 = 1\,; \tag{11.14}$$

$$\ddot{\boldsymbol{x}} - \boldsymbol{x}'' = 0\,. \tag{11.15}$$

The physical meaning of these equations can be easily understood. The first of eqs. (11.14) says that the vector $\dot{\boldsymbol{x}}$ is perpendicular to the string and thus represents the physically observable velocity, $\boldsymbol{v}_\perp$. The second constraint equation can be written as $\mathrm{d}\zeta = (1-\dot{\boldsymbol{x}}^2)^{-1/2}\,|\mathrm{d}\boldsymbol{x}| = \mathrm{d}M/\mu$, where

$$M = \mu \int (1-\dot{\boldsymbol{x}}^2)^{-1/2}\,\mathrm{d}\ell = \mu \int \mathrm{d}\zeta \tag{11.16}$$

is the energy (mass) of the string [compare with eq. (11.5)]. Thus we have chosen ζ to be proportional to the mass of string (counted from some arbitrary point on the string). For a closed loop ζ changes from 0 to M/μ around the loop, where M is the total mass of the loop. Finally, eq. (11.15) tells us that the acceleration of a string element in its local rest frame ($\dot{\boldsymbol{x}} = 0$) is inversely proportional to the local curvature radius, $R = |\mathrm{d}^2\boldsymbol{x}/\mathrm{d}\ell^2|^{-1}$. The direction of $\ddot{\boldsymbol{x}}$ is such that a curved string tends to straighten out. (Of course in doing so, it develops a velocity and therefore keeps oscillating.)

The general solution of eq. (11.15) is

$$\boldsymbol{x}(\zeta, t) = \tfrac{1}{2}[\boldsymbol{a}(\zeta - t) + \boldsymbol{b}(\zeta + t)]\,, \tag{11.17}$$

and eqs. (11.14) give the following constraints for the otherwise arbitrary functions $\boldsymbol{a}$ and $\boldsymbol{b}$:

$$\boldsymbol{a}'^2 = \boldsymbol{b}'^2 = 1\,. \tag{11.18}$$

The energy-momentum tensor of a moving string is [39]

$$T^{\mu\nu}(r, t) = \mu \int d\zeta \, (\dot{x}^\mu \dot{x}^\nu - x'^\mu x'^\nu) \, \delta^{(3)}(r - x(\zeta, t)) \tag{11.19}$$

and the angular momentum is

$$J = \mu \int d\zeta \, x(\zeta, t) \times \dot{x}(\zeta, t) \tag{11.20}$$

(in the gauge (11.14)).

12. Oscillating loops

The motion of a closed loop in its center-of-mass frame is described by a solution of the form (11.17), (11.18), where $a(\zeta)$ and $b(\zeta)$ are periodic functions with period $L = M/\mu$ and M is the mass of the loop:

$$a(\zeta + L) = a(\zeta); \qquad b(\zeta + L) = b(\zeta). \tag{12.1}$$

It is clear from eq. (11.17) that the motion of the loop must also be periodic in time with the same period. In fact the actual period is twice shorter, $T = L/2$ rather than $T = L$, since it is easily seen that [40]

$$r(\zeta + L/2, t + L/2) = r(\zeta, t). \tag{12.2}$$

An interesting property of the loop solutions is that, in the generic case, the string reaches the velocity of light at some points at certain moments during the period [39]. From eq. (11.17) we have

$$\dot{r}^2(\zeta, t) = \tfrac{1}{4}[a'(\zeta - t) - b'(\zeta + t)]^2. \tag{12.3}$$

Now, it follows from (11.18) and (12.1) that the vectors $a'(\zeta)$ and $-b'(\zeta)$ describe closed curves on a unit sphere as ζ runs from 0 to L. In the generic case, these two curves will have two or more intersections. [Note that since $\int a' \, d\zeta = \int b' \, d\zeta = 0$, neither of the two curves can completely lie in one hemisphere of the unit sphere.] Let $\zeta = \zeta_0$ be one of such points, $a'(\zeta_0) = -b'(\zeta_0)$. Then

$$\dot{r}^2(\zeta_0, nL) = 1, \tag{12.4}$$

where n is an integer.

We now turn to specific examples of loop trajectories. The periodic functions a and b can be expanded in Fourier series; then the constraints (11.18) give nonlinear algebraic equations for the coefficients. Exact solutions can easily be obtained in which only a few lowest frequencies are present. Several families of such solutions have been found by Kibble and Turok [40] and by Turok [39]. The simplest type of solution involving only one frequency is

$$x(\zeta, t) = \frac{L}{4\pi}\{\hat{e}_1(\sin\sigma_- + \sin\sigma_+) - \hat{e}_2(\cos\sigma_- + \cos\phi\cos\sigma_+) - \hat{e}_3\sin\phi\cos\sigma_+\}, \tag{12.5}$$

where

$$\sigma_\pm = \frac{2\pi}{L}(\zeta \pm t), \tag{12.6}$$

$\hat{e}_i$ are unit vectors in the directions of the Cartesian axes, and ϕ is a constant parameter. Rotating the coordinate frame by an angle $\phi/2$ around the direction of $\hat{e}_1$ and performing simple trigonometric transformations we bring eq. (12.5) to the form

$$x = \frac{L}{2\pi}\{\hat{e}_1\sin\sigma_1\cos\sigma_0 + \hat{e}_2\cos\frac{\phi}{2}\cos\sigma_1\cos\sigma_0 + \hat{e}_3\sin\frac{\phi}{2}\sin\sigma_1\sin\sigma_0\}, \tag{12.7}$$

where $\sigma_0 = 2\pi t/L$, $\sigma_1 = 2\pi\zeta/L$. At $t = 0$, the loop has the shape of an ellipse in the xy-plane. It rotates and stretches into a double line along the z-axis at $t = L/4$. At this moment the ends of the double line are moving in the x-direction with the velocity of light. At $t = L/2$ the loop returns to the elliptical shape and then goes through the cycle again. The parameter ϕ takes values from 0 to π. $\phi = 0$ corresponds to a circular loop which reaches the velocity of light as it collapses to a point. $\phi = \pi$ corresponds to a double line rotating in the (xz)-plane, its ends always moving with the velocity of light.

As we shall see in the next section, self-intersecting loops can intercommute and break into smaller pieces. If all loop trajectories intersect themselves at some point during the period, then the loop will rapidly decay into a cascade of smaller and smaller loops. Here, an important result has been obtained by Kibble and Turok who have found a class of loop trajectories which never self-intersect.

It is easily checked that adding to (12.5) terms in $\cos 2\sigma_\pm$ and $\sin 2\sigma_\pm$ does not yield any extra solutions. The next simplest solutions involve $\cos 3\sigma_\pm$ and $\sin 3\sigma_\pm$ [40]:

$$x = \frac{L}{4\pi}\{\hat{e}_1[(1-\alpha)\sin\sigma_- + \tfrac{1}{3}\alpha\sin 3\sigma_- + \sin\sigma_+]$$

$$- \hat{e}_2[(1-\alpha)\cos\sigma_- + \tfrac{1}{3}\alpha\cos 3\sigma_- + \cos\sigma_+] - 2\hat{e}_3[\alpha(1-\alpha)]^{1/2}\cos\sigma_-\}. \tag{12.8}$$

Kibble and Turok have shown that for $0 < \alpha < 1$ these loops never intersect themselves. The projection of one such loop ($\alpha = 0.7$) on the xy-plane is shown in fig. 1 at times $t = 0$ and $t = L/4$. At $t = L/4$ the loop develops two cusps and the velocity of light is reached at the peaks. (All loop solutions studied so far, excluding degenerate cases like a circular loop, develop cusps at the points of luminal motion.)

Turok [39] has studied a larger, two-parameter family of solutions with trigonometric functions of $\sigma_\pm$ and $3\sigma_\pm$ and has found that a large fraction of the parameter space is occupied by never-self-intersecting loops. To make this statement precise, one has to define a measure in the parameter space corresponding to the actual distribution of loop configurations formed in the early universe. This has not yet been done. At this time we can only say that the results of refs. [39, 40] do suggest that a substantial fraction of loop trajectories never self-intersect. The decay mechanisms for such loops are discussed in sections 14 and 15.

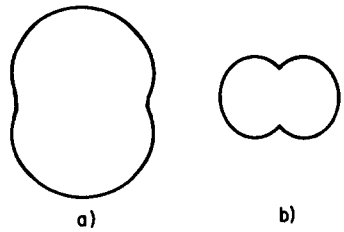

Fig. 1. The xy-projection of the loop (12.8) with $\alpha = 0.7$ (a) at $t = 0$ and (b) at $t = L/4$.

13. Intercommuting

Intersecting strings can intercommute [3] (or change partners) as shown in fig. 2. This process plays a crucial role in the evolution of strings, and it is important to know the intercommuting probability, p. Strings are described by classical solutions of the field equations, and one can expect that their intercommuting occurs at the classical level as well. Then the intercommuting process is totally deterministic, and the word "probability" refers to averaging over collision angles and relative velocities of the strings.

It appears that the only way to estimate p is to find numerical solutions of the nonlinear field equations describing colliding strings. Such an analysis has been recently done by Shellard [42] for the case of global strings of the model (7.1). He considered two strings at right angles moving towards one another with a relative velocity up to $0.5\,c$. The result is that the strings intercommute in all cases considered. It may well be that intercommuting is angle- and model-dependent, but these results do suggest that intersecting strings intercommute with high probability.

Shellard has also studied intercommuting of walls with walls bounded by strings (see fig. 3). The result is, again, that intercommuting occurred in all cases considered.

Let us consider the effects of intercommuting on oscillating loops of strings. If a loop of mass M self-intersects, it breaks into two loops, which we shall assume to have roughly equal masses. These daughter loops can be of self-intersecting or non-intersecting varieties, and we can introduce the probability, w, for a loop to be non-intersecting. Let us first consider the case when $w \approx 0$ and the loops rapidly decay into a cascade of smaller and smaller loops. When the size of the loops becomes comparable to the string width $\delta \sim \eta^{-1}$ (their mass being $\sim\eta$), they decay into elementary particles.

At each intercommuting, a certain fraction f of the energy of the splitting loop will go into the kinetic energy of daughter loops. Thus, after n splittings we have $\sim 2^n$ loops of energy

$$\varepsilon_n \sim 2^{-n} M \tag{13.1}$$

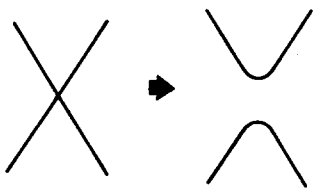

Fig. 2. Intercommuting strings.

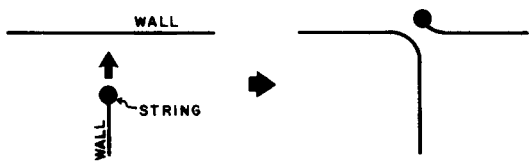

Fig. 3. A wall bounded by string intercommutes with another domain wall.

and rest mass

$$m_n \sim ((1-f)/2)^n M . \tag{13.2}$$

The loops decay when $m_n \sim \eta$, and the number of steps required is

$$n_* \sim \frac{\ln(M/\eta)}{\ln(2/(1-f))} . \tag{13.3}$$

If f is not too small ($f > n_*^{-1}$) the smallest loops and the resulting particles will be extremely relativistic:

$$\gamma_n \sim \varepsilon_n / m_n \sim (1-f)^{-n} . \tag{13.4}$$

The oscillation period of the loops in their respective rest frames is $t_n^{(0)} \sim m_n/2\mu$, but in the frame of the initial loop $t_n \sim \gamma_n t_n^{(0)} \sim 2^{-n} M/2\mu$. Hence the timescale of the whole decay process is

$$t \sim \sum_{n=0}^{n_*} t_n \sim M/\mu . \tag{13.5}$$

Let us now turn to the case when there is a nonzero probability for daughter loops to form in non-intersecting configurations, $w \neq 0$. Partial decay of an ensemble of loops with initial masses $\sim M$ will then give rise to a spectrum of non-intersecting loops with masses $\lesssim M$. The average number of loops with mass $\sim 2^{-n}M$ is $\sim 2^n(1-w)^n wN$, where N is the number of original loops. (Smaller loops of the spectrum will be relativistic, and $2^{-n}M$ should be regarded as their energy, not the rest mass.) The fraction of total mass carried by such loops is $\sim w(1-w)^n$. For w not too small, most of the mass is in the loops comparable in size to the original ones.

14. Gravitational radiation from loops

The dominant energy-loss mechanism for non-intersecting loops is the gravitational radiation. Loops of size R have a typical frequency $\omega \sim R^{-1}$, and one can estimate the radiation rate using the quadrupole formula [12]:

$$\mathrm{d}M/\mathrm{d}t \sim -GM^2R^4\omega^6 \sim -G\mu^2 . \tag{14.1}$$

Here, $M \sim \mu R$ is the mass of the loop. The lifetime of the loop is then

$$\tau \sim M/|\dot{M}| \sim R/G\mu . \tag{14.2}$$

If the energy scale of strings is $\eta \ll m_p$, where $m_p \sim 10^{19}$ GeV is the Planck mass, then

$$G\mu \sim (\eta/m_p)^2 \ll 1 . \tag{14.3}$$

For a typical grand unification energy scale, $\eta \sim 10^{16}$ GeV and $G\mu \sim 10^{-6}$.

The motion of loops is relativistic, and we have seen that at one moment during the period certain points of the loop actually reach the velocity of light. This indicates that the quadrupole formula is quantitatively incorrect. A more reliable estimate of the radiation rate can be obtained using the following general equations [43]

$$\frac{dP}{d\Omega} = \sum_{n=1}^{\infty} \frac{dP_n}{d\Omega} \tag{14.4}$$

$$\frac{dP_n}{d\Omega} = \frac{G\omega_n^2}{\pi} \{T^*_{\mu\nu}(\omega_n, \boldsymbol{k})\, T^{\mu\nu}(\omega_n, \boldsymbol{k}) - \tfrac{1}{2}|T^{\nu}_{\nu}(\omega_n, \boldsymbol{k})|^2\}\,. \tag{14.5}$$

Here, $dP_n/d\Omega$ is the intensity of radiation at frequency $\omega_n = 4\pi n/L$ per unit solid angle in the direction of $\boldsymbol{k}$, $|\boldsymbol{k}| = \omega_n$ and

$$T^{\mu\nu}(\omega_n, \boldsymbol{k}) = \frac{2}{L}\int dt \exp(i\omega_n t) \int d^3x \exp(-i\boldsymbol{k}\cdot\boldsymbol{x})\, T^{\mu\nu}(\boldsymbol{x}, t) \tag{14.6}$$

is the Fourier transform of the string energy-momentum tensor (11.19). Equations (14.4)–(14.6) give the gravitational radiation from a periodic source with period $T = L/2$ to the lowest order in G and without any further assumptions about the source. The total power of the radiation is

$$\dot{M} = -\sum_n P_n\,. \tag{14.7}$$

Turok [39] has applied this formalism to simple string configurations which, however, have little resemblance to actual loop trajectories. A numerical calculation of the radiated power for the exact loop solutions found by Kibble and Turok has been done in ref. [41]. Here we shall summarize the results.

The energy loss per unit time by an oscillating loop is given by

$$\dot{M} = -\gamma G\mu^2\,, \tag{14.8}$$

where γ depends on the particular loop trajectory, but is typically ~ 100. Figure 4 shows γ as a function

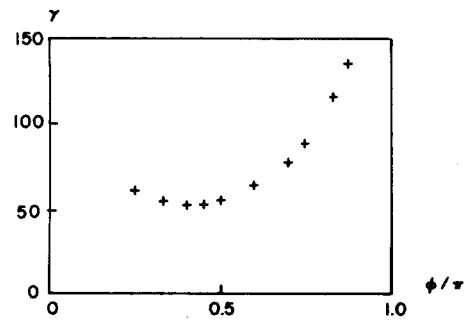

Fig. 4. Gravitational radiation power for the family of loops (12.7).

of the parameter ϕ for the family of solutions (12.5). The minimal value of γ in this family of loops is ~ 50. Similar results are obtained for non-intersecting loops found in refs. [39, 40]. The large values of γ are partly due to the significant contribution of high frequencies.

An asymmetric loop configuration can radiate momentum and accelerate like a rocket. A numerical calculation for several asymmetric loops gives [41] $|\dot{P}| \sim 10\, G\mu^2$. With such an acceleration, a loop would develop a velocity $v \sim (\dot{P}/M)\,\tau \sim 0.1$ by the end of its lifetime. However, due to angular momentum radiation, the direction of $\dot{P}$ gradually changes. With $\dot{L} \sim G\mu^2 R$, the loop rotates by $\sim \pi$ in $\Delta t \sim (G\mu)^{-1/2} R$. The velocity developed in time Δt is $\sim (G\mu)^{1/2}$. Besides, in the cosmological context, the "gravitational rocket" effect is counteracted by the gravitational drag due to small-angle scattering of particles [20, 21].

15. *Electromagnetic radiation*

For macroscopically large loops, only emission of massless particles can be important. If R is the size of the loop, then its typical frequency of oscillation is $\omega \sim R^{-1}$, and the emission of particles with masses greater than R^{-1} is suppressed. Assuming that neutrinos have nonvanishing masses, the only process competing with the gravitational radiation for macroscopic loops is the electromagnetic radiation.

The strings are characterised by the expectation values of a Higgs field ϕ and a gauge field W_μ. Since $\langle\phi\rangle$ is invariant under operations of the unbroken subgroup H, including the electromagnetic gauge transformations, it follows that ϕ is electrically neutral and does not couple to the electromagnetic field A_μ. Couplings of the form W^2A and W^3A are also absent [44] because of the antisymmetry of the group structure constants. Thus there is no interaction term coupling a single photon field to the fields of the string. Two-photon emission can occur due to the quartic couplings, W^2A^2, and this is the dominant radiation mechanism. (Couplings of this form are present if the generators corresponding to the fields W_μ and A_μ do not commute.) The corresponding diagrams are shown in fig. 5. The radiation rate has been estimated in ref. [44] by first studying the photon emission from small oscillations on straight strings (the small parameter being ωa, where a is the amplitude of oscillations) and then extrapolating the results to the case of large amplitudes ($\omega a \sim 1$). The result is

$$\dot{M}_\gamma \sim -R^{-2} \tag{15.1}$$

where R is the size of the loop. The answer is independent of the gauge coupling g, since the gauge field of the string is proportional to g^{-1}.

Photon emission can also occur due to vacuum polarization processes. An example of a diagram with a fermion loop is shown in fig. 6. Such diagrams turn out to be suppressed by powers of δ/R, where δ is the thickness of the string.

Comparing eq. (15.1) with the gravitational radiation rate (14.1), we see that for macroscopic loops of mass $M > m_p \sim 10^{-5}$ g the gravitational radiation is the dominant energy loss mechanism.

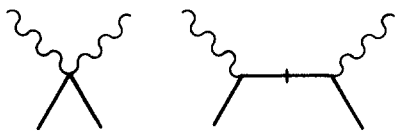

Fig. 5. Diagrams for two-photon emission from an oscillating string. The solid lines represent the classical gauge field of the string, the barred solid line represents other heavy gauge fields, and wavy lines represent photons.

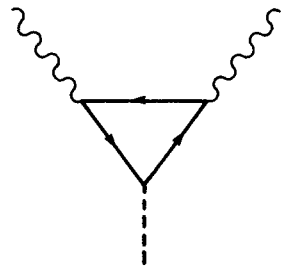

Fig. 6. Vacuum polarization diagram for electromagnetic radiation from a string. The dashed line represents the scalar Higgs field of the string, and the directed solid lines represent fermions.

16. Strings in expanding universe

In this section we shall derive the equations of motion and discuss the behavior of the strings in the Robertson–Walker metric (2.1). It will be convenient to use the conformal time variable τ, $d\tau = dt/a(t)$, so that the metric takes the form

$$ds^2 = a^2(\tau)(d\tau^2 - dx^2 - dy^2 - dz^2). \tag{16.1}$$

In a radiation-dominated universe ($a \propto t^{1/2}$) we have $\tau \propto t^{1/2}$, $a(\tau) \propto \tau$ and in a matter-dominated universe ($a \propto t^{2/3}$) $\tau \propto t^{1/3}$, $a \propto \tau^2$.

One can derive the equations of motion of a string from the action (11.3) and then try to solve them analytically or numerically. The case tractable analytically is that of small perturbations on a straight string.

Let us first choose the gauge

$$\zeta^0 = \tau, \qquad \zeta^1 = x \tag{16.2}$$

[compare with (11.9)] and assume for simplicity that the string moves in the (x, y)-plane, $z = 0$. Then the string trajectory is described by one function $y(x, \tau)$ and the string Lagrangian takes the form

$$L = -\mu[-g^{(2)}]^{1/2} = -\mu a^2(\tau)(1 + y'^2 - \dot{y}^2)^{1/2}, \tag{16.3}$$

where dots and primes represent derivatives with respect to τ and x respectively. The corresponding equation of motion is

$$\left(\frac{\partial}{\partial\tau} + 2\frac{\dot{a}}{a}\right)[\dot{y}(1 + y'^2 - \dot{y}^2)^{-1/2}] = \frac{\partial}{\partial x}[y'(1 + y'^2 - \dot{y}^2)^{-1/2}]. \tag{16.4}$$

Obviously, a straight line, $y = \text{const.}$, is a solution. A straight string remains straight and is simply stretched by expansion. Taking $y = 0$ as the unperturbed solution, we shall now consider small perturbations on a straight string.

In a radiation-dominated universe and assuming

$$y'^2, \dot{y}^2 \ll 1, \tag{16.5}$$

eq. (16.4) becomes

$$\ddot{y} + 2\tau^{-1}\dot{y} - y'' = 0 \tag{16.6}$$

and plane wave solutions of the form $y(\tau)\,e^{ikx}$ are easily found [38]:

$$y(\tau) = A_1\,\tau^{-1}\sin(k\tau)\,, \tag{16.7}$$

$$y(\tau) = A_2\,\tau^{-1}\cos(k\tau)\,. \tag{16.8}$$

Here, A_1 and A_2 are constant coefficients. It should be remembered that x and y are co-moving coordinates and $2\pi/k$ is the co-moving wavelength of the wave. The physical wavelength $\lambda = 2\pi\,a(\tau)/k$ grows proportionally to the scale factor. The quantity $k\tau \sim t/\lambda$ gives the ratio of the horizon size to the wavelength (by order of magnitude).

Let us first consider the case when both the wavelength and the amplitude of the wave on a string are much greater than the horizon: $k\tau \ll 1$, $A \gg \tau^2$. In this case, solutions (16.8) do not satisfy the conditions (16.5) and only solutions of the form (16.7) should be considered. In the limit $k\tau \to 0$, (16.7) reduces to a constant. The string does not move in co-moving coordinates, which means that it is being conformally stretched by the expansion: both amplitude and wavelength grow like $a(\tau)$, the shape of the string remaining unchanged.

Now consider the opposite limiting case when both the amplitude and the wavelength are smaller than the horizon: $k\tau \gg 1$, $A \ll \tau^2$. In this case, the wavelength still grows like $a(\tau)$, but the physical amplitude of the wave, $a(\tau)\,A\,\tau^{-1}$, remains constant. As the ratio of the amplitude to the wavelength decreases, the string becomes less and less curved. Similar results can be obtained in the general case of a power-law expansion: $a(\tau) \propto \tau^{\alpha}$ [47].

Extrapolating this perturbative analysis to the case of strongly curved strings, one expects that, in general, waves bigger than the horizon are conformally stretched, while the irregularities on scales smaller than the horizon are smoothed out [38, 12]. Numerical calculations of refs. [45, 46] are in qualitative agreement with this picture.

To give some examples of the behavior of strings in the early universe, first consider a circular loop of initial radius R_0 much greater than the horizon at time t_0, $R_0 \gg t_0$, assuming $a(t) \propto t^{1/2}$. The loop is stretched like the scale factor,

$$R(t) = (t/t_0)^{1/2} R_0 \tag{16.9}$$

until it comes within the horizon. This happens at $t = t_h$ such that $R(t_h) \sim t_h$:

$$t_h \sim R_0^2/t_0\,. \tag{16.10}$$

At this time, the radius of the loop begins to decrease. When the loop is much smaller than the horizon, effects of expansion are unimportant, and it collapses to a point with relativistic speed, just like it would in flat space–time.

As another illustration, consider a large irregular loop having overall size $R_0 \gg t_0$, but locally having the shape of a 3-dimensional random walk of step $\xi_0 \sim t_0$. Then the initial total length of the loop is $\ell_0 \sim R_0^2/\xi_0$. (As we shall see later, strings formed at a phase transition in the early universe have

Brownian shapes.) In the course of expansion the size of the loop is conformally stretched like in eq. (16.9) until the loop becomes smaller than the horizon at $t \sim t_h$. Since irregularities on scales smaller than the horizon are smoothed out, at any time $t \ll t_h$ the loop has the shape of a random walk of step $\xi \sim t$, and its length is

$$\ell(t) \sim R^2(t)/t \sim \text{const}. \tag{16.11}$$

if the universe is radiation-dominated, and

$$\ell(t) \propto t^{1/3} \tag{16.12}$$

in a matter-dominated universe. By the time the loop comes within the horizon it loses its Brownian appearance and is relatively smooth. When the size of the loop is much smaller than the horizon, effects of expansion can be neglected, and we have a regular oscillating loop.

To conclude this section, I would like to give another form of the equations of motion for a string in expanding universe, which is useful for computer calculations. A convenient choice of gauge is

$$\zeta^0 = \tau, \qquad \dot{\boldsymbol{x}} \cdot \boldsymbol{x}' = 0 \tag{16.13}$$

and the equations of motion in this gauge are [45]

$$\dot{\boldsymbol{v}} + 2(\dot{a}/a)(1 - v^2)\boldsymbol{v} = \varepsilon^{-1}(\varepsilon^{-1}\boldsymbol{x}')' \tag{16.14}$$

$$\dot{\varepsilon} = -2(\dot{a}/a)\varepsilon v^2 . \tag{16.15}$$

Here, $\boldsymbol{v} = \dot{\boldsymbol{x}}$, $\varepsilon = |\boldsymbol{x}'|(1 - v^2)^{-1/2}$, dots and primes are derivatives with respect to τ and ζ, respectively. Equation (16.15) is not an independent equation; it follows from eqs. (16.14) and (16.13). This equation describes how the energy of the string

$$M(\tau) = \mu\, a(\tau) \int \varepsilon \, \mathrm{d}\zeta , \tag{16.16}$$

changes with time. If the string is practically at rest with respect to local co-moving frames ($\boldsymbol{v} = 0$), $\varepsilon \approx$ const. and its mass grows like $a(t)$. For a rapidly moving string ε decreases and the rate of growth of the energy is reduced. This can be understood in terms of the usual redshift of the kinetic energy in expanding universe.

Note that eqs. (16.13) do not fix the gauge completely. The remaining gauge freedom includes reparametrizations of the form $\zeta \to \tilde{\zeta}(\zeta)$. In flat space–time ($\dot{a} = 0$) $\dot{\varepsilon} = 0$, and eqs. (11.14), (11.15) are obtained from (16.14), (16.15) if we choose $\varepsilon = 1$. It is clear that the gauge (11.14) cannot be imposed in expanding universe, since the second of eqs. (11.14) is inconsistent with (16.15). Equation (16.14) was used in the computer calculations of refs. [45, 46].

17. Dynamics of global strings

As shown in section 7, the mass per unit length of a straight global string is

$$\mu \approx 2\pi \eta^2 \ln(R/\delta) \tag{17.1}$$

and diverges in the limit of an infinite cut-off radius R. If we have two parallel strings with opposite sense of $\Delta\theta$ (so that $\Delta\theta = 0$ for a contour enclosing both strings), then the role of the cut-off radius is played by the distance between the strings, and the two strings are attracted to one another with a force (per unit length)

$$F = \partial\mu/\partial R \approx 2\pi\eta^2/R\,. \tag{17.2}$$

This force can be thought of as due to the interaction of strings with a long-range Goldstone field, θ. Strictly speaking, both the Goldstone field and the string are described by the same complex field ϕ with the Lagrangian (7.1). However, for macroscopic strings, it may be possible to represent this Lagrangian as a sum of real scalar field (θ) and string terms plus an interaction term. To my knowledge, this has not been done, and I am not aware of any quantitative results on the dynamics of global strings. Some qualitative conclusions concerning the evolution of global strings can still be reached using the following observation.

We shall see in chapter 4 that cosmological strings have Brownian shapes with typical curvature radii comparable to the distance between the strings. The force per unit length due to tension in curved strings is $F \sim \mu/R$ and is greater than the interaction force (17.2) by a large factor $\ln(R/\delta) \sim 100$. This suggests that the dynamics of global strings is dominated by tension, and thus should not be much different from that of local strings. The main difference can be expected in the behavior of closed loops. In the case of global strings, closed loop trajectories are probably not periodic, and there may be no loops which never intersect themselves. String configurations corresponding to non-intersecting loops of local strings will be gradually modified by the force of interaction between different parts of the loop, and may intersect themselves after ~ 100 oscillations. Thus, one's best guess seems to be that the lifetime of global string loops is

$$\tau \sim 100R\,. \tag{17.3}$$

18. Dynamics of domain walls

The action for a domain wall can be derived in the same manner as the string action in section 11:

$$S = -\sigma \int [g^{(3)}]^{1/2}\, \mathrm{d}^3\zeta\,. \tag{18.1}$$

Here, σ is the wall tension, ζ^0, ζ^1 and ζ^2 are arbitrary parameters on the wall and $g^{(3)}$ is the determinant of the metric tensor on the 3-dimensional hypersurface described by the wall in space–time, $g^{(3)}_{ab} = g_{\mu\nu}\, x^{\mu}_{,a}\, x^{\nu}_{,b}$. It can be shown that eq. (18.1) is equivalent to

$$S = -\sigma \int \mathrm{d}t \int \mathrm{d}S\, (1 - v_{\perp}^2)^{1/2}\,, \tag{18.2}$$

where $v_{\perp}$ is the transverse velocity of the wall and $\mathrm{d}S$ is the surface element.

We can use the gauge freedom $\zeta^a \to \tilde{\zeta}^a(\zeta)$ to fix the parameters ζ^a as

$$\zeta^a = t, \qquad \zeta^1 = x, \qquad \zeta^2 = y. \tag{18.3}$$

Then the motion of the wall is described by one function $z(x, y, t)$ and the action takes the form (in flat space–time)

$$S = -\sigma \int\int\int dt\, dx\, dy\, (1 + z_x'^2 + z_y'^2 - \dot{z}^2)^{1/2}. \tag{18.4}$$

The corresponding equation of motion is

$$\frac{\partial}{\partial t}(\gamma \dot{z}) - \frac{\partial}{\partial x}(\gamma z_x') - \frac{\partial}{\partial y}(\gamma z_y') = 0 \tag{18.5}$$

where $\gamma = (1 + z_x'^2 + z_y'^2 - \dot{z}^2)^{-1/2}$. It is easily checked that

$$z = f(x \pm t) \tag{18.6}$$

solves eq. (18.5) for arbitrary f. Such solutions describe plane waves of arbitrary shape propagating on the wall with the velocity of light.

The equation of motion for a wall in expanding universe (16.1) is

$$\left(\frac{\partial}{\partial \tau} + 3\frac{\dot{a}}{a}\right)(\gamma \dot{z}) - \frac{\partial}{\partial x}(\gamma z_x') - \frac{\partial}{\partial y}(\gamma z_y') = 0. \tag{18.7}$$

For small perturbations on a straight wall, $z = z(\tau)\exp(i\boldsymbol{k}\cdot\boldsymbol{x})$, eq. (18.7) takes the form

$$\ddot{z} + 3(\dot{a}/a)\dot{z} + k^2 z = 0. \tag{18.8}$$

As in the case of strings, it can be shown that waves greater than the horizon are conformally stretched ($z(\tau) \approx$ const.) and waves smaller than the horizon are smoothed out ($z(\tau) \propto a^{-3/2}$) [47].

19. *Gravitational field of strings and walls*

The gravitational field of strings and vacuum domain walls is very different from that of regular massive rods and planes [14]. The difference is easily understood if we note that for a static matter distribution with energy-momentum tensor

$$T_\mu^\nu = \mathrm{diag}(\rho, -P_1, -P_2, -P_3) \tag{19.1}$$

the correct Newtonian limit of Einstein's equations is

$$\nabla^2\phi = 4\pi G(\rho + P_1 + P_2 + P_3). \tag{19.2}$$

For nonrelativistic matter $P_i \ll \rho$ and $\nabla^2\phi = 4\pi G\rho$. The energy-momentum tensor of a straight string (5.10) has $P_1 = P_2 = 0$, $P_3 = -\rho$, and eq. (19.2) suggests that straight strings produce no gravitational force on surrounding matter. For a domain wall [see eq. (4.5)] $P_1 = P_2 = -\rho$, $P_3 = 0$ and eq. (19.2) gives $\nabla^2\phi = -4\pi G\rho$, indicating that the gravitational field of domain walls is repulsive.

The solution of Einstein's equations for a string has been found in ref. [14] assuming that the parameter $G\mu$ is small, which is the physically interesting case (μ is the string tension). Large values of $G\mu$ and the internal metric of the string are discussed in ref. [16]. Outside the string core the metric is

$$ds^2 = dt^2 - dz^2 - dr^2 - (1 - 4G\mu)^2 r^2 d\phi^2 . \tag{19.3}$$

A coordinate transformation $\phi' = (1 - 4G\mu)\phi$ brings the metric to a locally Minkowskian form, but now the angle ϕ' changes from 0 to $(1 - 4G\mu)2\pi$. Thus, eq. (19.3) describes a "conical space", that is, a flat space with a wedge of angular size $8\pi G\mu$ taken out and the two faces of the wedge identified. In the coordinates (t, z, r, ϕ') the geodesics are just straight lines, and we see immediately that a particle initially at rest relative to the string will remain at rest and will not experience any gravitational attraction.

Although the metric (19.3) is locally flat, its global structure is different from that of Minkowsky space. The most striking effect of this difference is the formation of double images of objects located behind the string [14]. This is illustrated in fig. 7. The light rays from the quasar intersect behind the string and the observer sees two images of the quasar. If ℓ and d are the distances from the string to the quasar and to the observer, respectively, then the angular separation between the images is [15, 16]

$$\delta\phi = 8\pi G\mu\ell(d + \ell)^{-1} \tag{19.4}$$

assuming that $G\mu \ll 1$ and that the string is perpendicular to the line of sight.

Gravitational lensing by a string is a classical analogue of the Aharonov–Bohm effect [48]. Space–time curvature is confined to the string core, but its effect is "felt" by the photons propagating in flat space–time region around it. As in the Aharonov–Bohm case, a Minkowskian coordinate system can be chosen in any region on one side of the string, but such systems do not exist in regions surrounding the string.

It should be emphasized that all this discussion applies only to portions of strings which can be regarded as straight. A closed loop of size R produces a regular Schwarzschild field at distances $\gg R$.

The solution of Einstein's equations for a plane domain wall with energy-momentum tensor

$$T^{\nu}_{\mu} = \sigma\,\mathrm{diag}(1, 1, 1, 0)\,\delta(z) \tag{19.5}$$

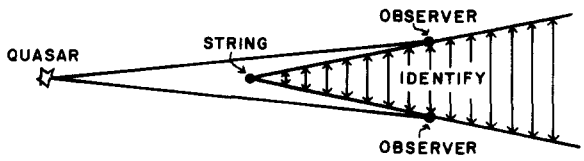

Fig. 7. The conical space around a straight string can be obtained from a Euclidean space by cutting out a wedge of angular size $8\pi G\mu$ and identifying the exposed surfaces. Light rays emitted by the quasar intersect behind the string, and the observer sees two images of the same quasar.

has been found in refs. [49, 50]:

$$ds^2 = (1-\kappa z)^2\,dt^2 - dz^2 - (1-\kappa z)^2\,e^{2\kappa t}(dx^2+dy^2)\,, \tag{19.6}$$

where $\kappa = 2\pi G\sigma$. Note that this solution is time-dependent: no static solutions with T^{ν}_{μ} of the form (19.5) exist. In the plane of the wall ($z=0$) the metric is that of a $(2+1)$-dimensional de Sitter space, while the (z, t) part of eq. (19.6) is the $(1+1)$-dimensional Rindler metric describing a flat space in the frame of reference of a uniformly accelerated observer. An observer at $z=0$ will see test particles moving away from the wall with acceleration $a = \kappa = 2\pi G\sigma$, in agreement with the Newtonian analysis.

The metric (19.6) has an event horizon: an observer at $z=0$ never sees particles and light cross the surfaces $z = \pm\kappa^{-1}$. On the other hand, it takes a finite proper time for a particle to reach $|z| = \kappa^{-1}$. In addition, usual de Sitter horizons of radius κ^{-1} exist in the (xy)-plane. The singularity at $|z| = \pm\kappa^{-1}$ is not a true singularity of the metric. In fact, it can be shown that the metric (19.6) is locally flat everywhere except on the wall itself.

Just like in the case of strings, it is important to realize that these results can be applied directly only to plane domain walls. The gravitational field of curved, and especially closed walls can be very different. For example, the gravitational field outside a collapsing spherical wall [50] is described by the Schwarzschild metric.

20. Interaction with particles

To analyze the cosmological evolution of topological defects, it is important to know the force of friction experienced by moving walls and strings due to their interaction with particles.

A domain wall is transparent to some particles, but may be a nearly perfect reflector for some other particles. The wall is formed when the temperature of the universe is $T \sim \eta$, where $\langle\phi\rangle = \eta$ is the VEV of the corresponding scalar field. At later times, when $T \ll \eta$, the typical wavelength of the particles, $\lambda \sim T^{-1}$, is much greater than the thickness of the wall, $\delta \sim \eta^{-1}$; hence we can treat the wall as infinitely thin. Consider a multiplet of fields ψ_a such that the VEV of ϕ gives masses $\sim\eta$ to some members of the multiplet, other members remaining massless. In general, different components of ψ_a will acquire masses on the two sides of the wall (since the VEVs of ϕ are different). Everett has shown [51] that for the components whose mass changes across the wall the probability of reflection is large (provided that $\lambda \gg \delta$).

We can now estimate the force of friction acting on a domain wall moving with velocity v relative to the radiation. For simplicity we shall assume that the wall is not ultrarelativistic, so that $(1-v^2)^{-1/2} \sim 1$. The density of particles per spin degree of freedom is $n \sim \pi^{-2}T^3$, the average momentum transfer per collision is $\sim Tv$, and we can write for the force per unit area of the wall [3]

$$F_w \sim N_w n T v \sim \pi^{-2} N_w T^4 v\,, \tag{20.1}$$

where N_w is the number of particle states changing their mass across the wall.

Scattering of particles on strings has been studied by Everett [52]. He considered a particle multiplet ψ_a with a mass matrix $M^2_{ab}(\theta)$ changing around the string. Heavy fields of the multiplet have masses $\sim\eta$ and are absent from the thermal bath at $T \ll \eta$. Everett has found that the scattering cross-section of light members of the multiplet per unit length of the string is given by

$$\sigma \sim \pi^2/k \ln^2(k\delta) \tag{20.2}$$

and is practically insensitive to the internal structure of the string. Here, k is the momentum of the particle ($k \sim T$) and δ is the width of the string ($\delta \sim \eta^{-1}$). The force of friction per unit length of a moving string is then [52]

$$F_s \sim N_s T^3 v/\ln^2(T\delta), \tag{20.3}$$

where N_s is the number of light particles interacting with the fields of the string.

Finally, to discuss the evolution of monopoles connected by strings, we shall need the force of friction acting on a moving monopole. This is given by [10]

$$F_m \sim T^2 v. \tag{20.4}$$

4. Evolution of topological defects

21. Domain walls

In this section, we shall discuss the configuration of the domain walls at the time of formation and their further cosmological evolution. The initial shape of the walls right after the phase transition is determined by the random variation of the scalar VEV, $\langle\phi\rangle$. Hence, one expects the walls to be very irregular, random surfaces with a typical curvature radius $\sim\xi$, where ξ is the correlation length of $\langle\phi\rangle$. To learn more about the system of walls at formation, one can use a Monte Carlo simulation [53, 54].

Take a cubic volume of size $N\xi$ divided into N^3 cubic cells and assign to each cell a number $+1$ or -1 [corresponding to $\langle\phi\rangle = \pm\eta$ in the model (4.1)] at random with equal probability. We shall call the corresponding cells plus-cells and minus-cells, respectively. The walls lie on the boundaries between plus- and minus-cells.

To characterize the system of domain walls, one can look for the size distribution of clusters of connected plus-cells. (Two cells are connected if they have a common face; the size of a cluster is the number of cells in the cluster.) Of course, the distribution of minus-cell clusters will be similar. This is a typical problem of percolation theory [55], which is concerned with statistical properties of systems like ours for various types of lattices at different concentrations of plus-cells, p. The central concept of percolation theory is the critical concentration, p_c, at which an infinite plus-cluster first appears (in an infinite lattice). The value of p_c is different for different lattices, but in all 3-dimensional cases it is smaller than 0.5. In our case, $p = 0.5$, and thus the system is above the percolation threshold. (For a cubic lattice, $p_c = 0.31$.)

The following facts are known about the properties of percolating systems at $p > p_c$: (1) there is only *one* infinite plus-cluster (and one infinite minus-cluster if $p < 1 - p_c$) and (2) the number density of finite clusters, n_s, decreases exponentially with their size, s:

$$n_s \propto s^{-\tau} \exp(-\alpha s^{2/3}). \tag{21.1}$$

Here, the numerical coefficients τ and α depend on p.

The implications of these results for the system of domain walls are straightforward. The system is

dominated by *one* infinite wall of very complicated topology [3]. In addition, there are some finite closed walls. Most of them have dimensions $R \sim \xi$. The probability of finding closed walls with $R \gg \xi$ exponentially decreases with R, $\ln n \propto -R^2$. In a typical simulation on a lattice of size $N = 40$, ~98% of all plus-cells and ~87% of the total wall area belong to the "infinite" cluster [54].

Once it is formed, how will the system of walls evolve? Tension in convoluted walls, σ, produces a force per unit area $f \sim \sigma/R$, where R is the mean curvature radius. As a result, isolated closed walls smaller than the horizon ($R \ll t$) will shrink and disappear. In vacuum, a collapsing closed wall would develop kinetic energy and would keep oscillating, just like a loop of string discussed in section 12. However, the motion of the walls is damped by the force of friction (20.1). Omitting numerical factors, the retarding force per unit area is $F_w \sim T^4 v \sim v/Gt^2$, where I have used

$$T^4 \sim \rho \sim 1/Gt^2 \tag{21.2}$$

[see eqs. (2.4), (2.8)]. For sufficiently large walls the velocity v is determined by the balance between tension and friction, $f \sim F_w$:

$$v \sim G\sigma t^2/R \tag{21.3}$$

and the typical dissipation time is

$$t_d \sim R/v \sim R^2/G\sigma t^2 . \tag{21.4}$$

When the wall shrinks to $R \sim G\sigma t^2$, its motion becomes relativistic, the energy loss rate is $\dot{M} \sim -F_w R^2 v$ and the energy of the wall is dissipated on a timescale $M/|\dot{M}| \sim G\sigma t^2$. From eq. (21.4) we see that closed walls of size smaller than

$$R(t) \sim (G\sigma)^{1/2} t^{3/2} \tag{21.5}$$

disappear in less than one Hubble time (t). Similarly, it can be argued [3] that small-scale irregularities of the infinite wall are damped out, so that the characteristic scale at time t is given by (21.5). The scale grows like $t^{3/2}$ and becomes comparable to the horizon at

$$t_* \sim (G\sigma)^{-1} . \tag{21.6}$$

The contribution of the walls to the energy density of the universe is $\rho_w \sim \sigma R^2/R^3 \sim \sigma/R$, so that for $t < t_*$,

$$\rho_w/\rho \sim (t/t_*)^{1/2} . \tag{21.7}$$

At $t \sim t_*$, $\rho_w \sim \rho$ and the universe becomes dominated by domain walls. For $t > t_*$, the curvature radius of the walls is greater than $(G\sigma)^{-1}$ and the metric near the walls is given by eq. (19.6). Space–time becomes very inhomogeneous and develops horizons at distances $\sim(G\sigma)^{-1}$ from the walls. A domain wall stretching across the present horizon would introduce a density fluctuation $\delta\rho/\rho \sim G\sigma t_{pres} \sim 10^{60}(\eta/m_p)^3$ and a comparable fluctuation in the temperature of the microwave background. Observations constrain $\delta T/T$ to be $\lesssim 10^{-4}$ and thus models predicting topologically stable domain walls with $\eta \gtrsim 10^{-2}$ GeV should be ruled out [9, 3].

This rule is not without exceptions. If the formation of domain walls is followed by inflation, the walls can be inflated away far beyond the present horizon.

As another example, consider the case when a discrete symmetry is broken at $T = T_1$ and then restored at $T = T_2$. An example of this sort was discussed at the end of section 9. In this case, the wall tension changes with temperature [14]. Omitting numerical factors and coupling constants,

$$\sigma \sim T^3, \tag{21.8}$$

and eq. (21.7) gives

$$\rho_w/\rho \sim (t_p/t)^{1/4} \tag{21.9}$$

where $t_p \sim 10^{-43}$ s is the Planck time. Hence, in models of this type, the universe never becomes wall-dominated.

Yet another possibility is to allow a small bias, so that one of the two vacuum states separated by the walls has slightly smaller energy density than the other: $\Delta\rho_v = \varepsilon \neq 0$ [9, 3]. This is the case of an approximate discrete symmetry. Regions of higher density vacuum tend to shrink, the corresponding force per unit area of the walls is $\sim\varepsilon$. The energy difference $\Delta\rho$ becomes dynamically important when this force becomes comparable to the force of tension, $f \sim \sigma/R$. For walls to disappear, this has to happen before the walls dominate the universe, that is, for $R < (G\sigma)^{-1}$. This requirement gives a lower bound for the asymmetry ε [14]

$$\varepsilon > G\sigma^2. \tag{21.10}$$

22. *Strings*

At the time of formation, one expects strings to have the shape of random walks of step $\sim\xi$ with a typical distance between the neighboring string segments also $\sim\xi$. Here, ξ is the correlation length of the Higgs field ϕ. The statistical properties of the system of strings at formation can be studied using a Monte Carlo simulation. This has been done in ref. [54] using the following prescription.

The simulation is done having in mind the U(1) model (5.2) in which the Higgs VEV is $\langle\phi\rangle = \eta\, e^{i\theta}$. The phase θ is randomly assigned at the vertices of a cubic lattice. For simplicity the phase at the vertices is allowed to take only three values: $\theta = 0, 2\pi/3, 4\pi/3$ (assuming that θ varies smoothly between the vertices). The size of the cubic cell is identified with the correlation length ξ. A string passes through the face of a cubic cell if θ changes by 2π when traced around the face. It can be checked that the construction is such that all strings are either closed or end at the boundaries of the lattice.

As expected, one finds [54] that long strings are Brownian, so that the length of string between two points separated by a distance $R \gg \xi$ is

$$\ell \sim R^2/\xi. \tag{22.1}$$

Results of the simulation for various sizes of the lattice indicate that a large fraction (~80%) of the total string length is due to infinite strings. The remaining strings are closed loops with a scale-invariant distribution

$$dn \sim R^{-4}\, dR . \tag{22.2}$$

Here, R is the characteristic size of the loop defined as $R = \Delta X_1 + \Delta X_2 + \Delta X_3$, where ΔX_i are the extents of the loop along the corresponding axes. The *length* of the loop is related to R by eq. (22.1). dn is the number of loops with sizes from R to $R + dR$ per unit volume.

We now turn to the evolution of the system of strings [3, 12, 38, 45, 54, 56, 57]. At very early times the motion of strings is heavily damped by the force of friction (20.3). For a rough estimate we can omit the numerical and logarithmic factors in eq. (20.3) and write

$$F_s \sim T^3 v . \tag{22.3}$$

Tension in convoluted strings produces a force per unit length $f \sim \mu/R$, where $\mu \sim \eta^2$ is the linear mass density (and tension) and R is the local curvature radius of the string. The velocity of the string is determined by $f \sim F_s$:

$$v \sim \mu/T^3 R . \tag{22.4}$$

(I am using Newtonian physics assuming $R \ll t$.) Small-scale irregularities on the strings are damped out by friction, and the typical curvature radius of strings at time t is $R(t) \sim vt$. Substituting this in eq. (22.4) and using eq. (21.2) we obtain

$$R(t) \sim (G\mu)^{1/2} (t/t_p)^{1/4} t . \tag{22.5}$$

Closed loops of size smaller than $R(t)$ shrink and disappear in less than one expansion time.

$R(t)$ becomes comparable to the horizon at

$$t_* \sim (G\mu)^{-2} t_p . \tag{22.6}$$

For $t > t_*$ the characteristic scale of the strings is $R(t) \sim t$. [Strings cannot be smoothed out on scales greater than t, since that would require superluminal velocities.] The force of tension is now $f \sim \mu/t$ and the force of friction is $F_s \sim (\mu/t)(t/t_*)^{-1/2}$. Hence, for $t \gg t_*$ the effects of friction become negligible. For a typical grand unified value $\eta \sim 10^{16}$ GeV we have $G\mu \sim 10^{-6}$ and $t_* \sim 10^{-31}$ s.

Expansion of the universe straightens out long strings on scales smaller than the horizon (so that the persistence length of Brownian strings is $\sim t$) and conformally stretches them on scales greater than the horizon. It has been shown in section 16 that the overall effect of expansion on large Brownian loops in a radiation-dominated universe is that the length (and therefore the mass) of the loop remains roughly constant. Similarly, it can be argued that the co-moving mass of infinite strings remains unchanged. This seems to indicate that the mass density of string scales like $\rho_s \propto a^{-3}$, while the radiation density is $\rho \propto a^{-4}$. Hence, $\rho_s/\rho \propto t^{1/2}$ and the universe becomes string-dominated. This, however, is *not* our final conclusion, since two important physical effects are still to be taken into account. These are intercommuting and gravitational radiation.

Pairs of strings intercommuting at two points can form closed loops. Loops can also be formed by self-intersection of individual strings (see fig. 8). These processes are important, since loops eventually radiate away their energy and save the universe from string domination.

Let $\nu(t)$ be the typical number of segments of infinite strings (or very large closed loops) per horizon

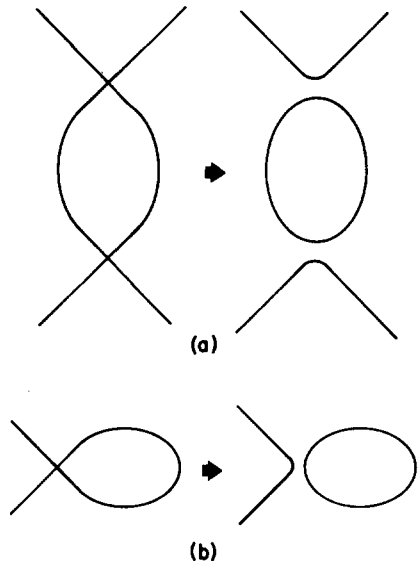

Fig. 8. Closed loop formation by intercommuting strings.

volume $\sim t^3$. Then the density due to infinite strings is $\rho_{\rm inf} \sim \nu\mu t^{-2}$ and each segment has about ν intersections per Hubble time. (At $t > t_*$ strings move with relativistic speeds, $v \sim 1$.) The total number of intersections in a volume t^3 per time interval dt is $\sim \nu^2 t^{-1}\, dt$ and the rate of loop formation per unit volume is

$$dn/dt \sim p\nu^2 t^{-4}. \tag{22.7}$$

Here, p is the probability of loop formation per intersection (it is, of course, related to the intercommuting probability). The typical curvature radius of strings at time t is $\sim t$, and we expect that loops formed by their intercommuting will have size $\sim t$. Then, by energy conservation, we must have

$$\frac{d\rho_{\rm inf}}{dt} + \frac{3}{2t}\rho_{\rm inf} \sim -\mu t \frac{dn}{dt}. \tag{22.8}$$

The second term on the left-hand side describes the dilution effect due to expansion, $a \propto t^{1/2}$. This equation does not take account of the effect inverse to the loop formation. If a segment of string intercommutes at one point with a closed loop, the loop gets absorbed into the segment. A more detailed analysis done by Kibble [56] indicates that inclusion of this effect does not change the qualitative conclusions. The reason is that the probability for a loop smaller than the horizon to be hit by a string rapidly decreases with time, and a large fraction of loops survive.

From eqs. (22.7) and (22.8) we obtain the following "kinetic" equation for $\nu(t)$:

$$d\nu/dt - \nu/2t \sim -p\nu^2/t. \tag{22.9}$$

We see that ν tends to decrease if $\nu \gg p^{-1}$ and tends to increase if $\nu \ll p^{-1}$. Thus, $\nu \sim p^{-1}$ is a stable solution.

With intercommuting probability ~1, it is natural to assume that $p \sim 1$. Then there are no more than a few segments of infinite strings per horizon volume at any time [3], and eq. (22.7) tells us that about one loop of size $\sim t$ is formed per horizon volume per Hubble time [12].

The density due to infinite strings is $\rho_{\text{inf}} \sim \mu/t^2$ and, using eq. (3.8),

$$\rho_{\text{inf}}/\rho \sim 30\, G\mu\,. \tag{22.10}$$

Let us now see what happens to the closed loops.

Loops of size R are formed at $t \sim R$. At that time, the number density of loops is (assuming $p \sim \nu \sim 1$ in eq. (22.7))

$$\mathrm{d}n(t \sim R) \sim R^{-4}\,\mathrm{d}R\,. \tag{22.11}$$

It is convenient to introduce the quantity

$$n_R = R\,\mathrm{d}n/\mathrm{d}R \tag{22.12}$$

which gives the number density of loops with sizes $\sim R$ in the interval $\Delta R \sim R$. Then eq. (22.11) gives $n_R(t \sim R) \sim R^{-3}$. At later times the loops are just diluted by the expansion:

$$n_R(t) \sim [a(R)/a(t)]^3\, R^{-3}\,. \tag{22.13}$$

During the radiation era, $a(t) \propto t^{1/2}$ and

$$n_R(t) \sim (tR)^{-3/2}\,. \tag{22.14}$$

The loops lose their energy by gravitational radiation and disappear with a typical lifetime

$$\tau \sim R/\gamma G\mu\,, \tag{22.15}$$

where γ is a numerical coefficient ~100 (see section 14). Hence, the loops surviving at time t have (initial) sizes greater than $\gamma G\mu t$. All smaller loops have already decayed. The mass density of loops at time t is

$$\rho_{\text{L}} \sim \int_{\gamma G\mu t}^{t} \mu\, R\, n_R(t)\,\frac{\mathrm{d}R}{R} \sim \gamma^{-1/2}\,(G\mu)^{1/2}\,(Gt^2)^{-1} \tag{22.16}$$

and, using eq. (3.8)

$$\rho_{\text{L}}/\rho \sim 30\,\gamma^{-1/2}\,(G\mu)^{1/2} \sim (G\mu)^{1/2}\,. \tag{22.17}$$

The dominant contribution to ρ_{L} is given by the smallest loops with $R \sim \gamma G\mu t$, which are about to decay. [In fact, the cut-off of the distribution (22.14) at $R \sim \gamma G\mu t$ is not sharp. It is easily understood that, for $R < \gamma G\mu t$, n_R is proportional to R, and thus $n_R(t)$ has a maximum at $R \sim \gamma G\mu t$.]

For closed loops formed during the matter-dominated era, $a \propto t^{2/3}$, eq. (22.13) gives

$$n_R(t) \sim (t^2 R)^{-1} \tag{22.18}$$

and we find, using eq. (3.12),

$$\rho_L/\rho \sim 6\pi G\mu \ln(\gamma G\mu)^{-1}. \tag{22.19}$$

The total mass density of strings is $\rho_s = \rho_{inf} + \rho_L$. From eqs. (22.10), (22.17), (22.19) and (14.3) it follows that $\rho_s/\rho \ll 1$ and the strings never dominate the universe. Unlike domain walls, strings do not cause cosmological trouble. In the following sections, we will see that strings can play a useful role in galaxy formation and can even produce some observable effects at present.

It should be noted that, in discussing the closed loops, I assumed that a large fraction of them is of non-self-intersecting variety. This is suggested by the results of Kibble and Turok [40] and Turok [39]. However, their results apply only to local strings. The motion of global string loops is not periodic, and they may frequently self-intersect (see section 17). In such a case, the lifetime of the loops will be short, and their contribution to the mass density will not be much different from that of infinite strings, so that $\rho_s/\rho \sim 30\, G\mu$. [If, as suggested in section 17, global strings self-intersect on a timescale $\tau \sim 100\, R$, then we obtain $\rho_s/\rho \sim 300\, G\mu$.]

Finally, it should be mentioned that the evolution of Z_n strings with $n > 2$ (see section 6) may be different from that described in this section. Such strings can form vertices where several strings join, and it appears that under the action of string tension, the vertices can reach equilibrium positions, so that the whole network will "freeze" with strings being stretched between the vertices by the expansion. In this case, the co-moving mass of strings will grow like $a(t)$ and the universe will eventually become string-dominated. The same conclusion applies to the case of non-commuting strings with a non-Abelian $\pi_1(M)$. For more discussion of a string-dominated universe, see section 28.

23. Walls bounded by strings

Walls bounded by strings are formed in two steps. Strings form at an earlier phase transition and evolve as discussed in the previous section. A later phase transition gives rise to walls which are bounded by strings, together with some closed walls. A numerical simulation of these phase transitions has been done in ref. [54] assuming that walls are formed soon after the string formation, so that the two correlation lengths are comparable. The results suggest that the system is dominated by one infinite cluster comprising about 90% of the total wall area and string perimeter. This cluster has a very complicated topology and is very "holey", so that its intersection with a plane gives a large number of short pieces. Some finite walls bounded by strings are also formed in numbers decreasing with their size. Closed domain walls are very rare. If the walls are formed much later than the strings, one has to take into account dynamical effects of the string evolution on scales smaller than the horizon. However, one expects that the results of ref. [54] still correctly represent the large-scale structure of the system.

The cosmological evolution of walls bounded by strings has been discussed in refs. [4–6]. Let μ and σ be the string and wall tensions, respectively. The force of tension in a string of curvature radius R, $f \sim \mu/R$, is greater than the wall tension, σ, for $R < \mu/\sigma$. Therefore, at $t < \mu/\sigma$ the evolution of strings will not be qualitatively different from that described in the previous section.

Walls are formed at $t_w \sim m_p/\eta_w^2$, which is earlier than $\mu/\sigma \sim \eta_s^2/\eta_w^3$ if $\eta_s > (m_p\eta_w)^{1/2}$. For definiteness, I shall assume that this is the case. (Here, η_s and η_w are the symmetry breaking scales corresponding to strings and walls, respectively, and I have omitted the coupling constant factor in σ.) Using eq. (22.6), it is easily checked that with this assumption friction of strings becomes unimportant at $t_* < \mu/\sigma$. For simplicity, we shall consider the case when the force of friction acting on domain walls is also negligible. This is so for axion models [5], both because the thickness of the wall is much greater than the thermal wavelength of the particles [51] and because the vacua on the two sides of the wall are identical, and particles do not change their masses across the wall (see section 20). The case where the wall friction is important is discussed in refs. [4, 6] with similar conclusions.

At $t > \mu/\sigma$ the typical curvature radius of the strings becomes greater than μ/σ, and the wall tension becomes dynamically important. Domain walls will tend to shrink pulling the strings toward one another, and the holes in the walls will increase in size. (This only applies to the holes of size greater than μ/σ. Smaller holes will tend to shrink and disappear.) The strings will frequently intersect and intercommute; as a result the wall connecting the strings is rapidly cut into pieces of size not much exceeding μ/σ. (I assume that the intercommuting probability is $p \sim 1$.)

A piece of wall of size $R > \mu/\sigma$ oscillates at a typical frequency $\omega \sim R^{-1}$ and loses its energy by gravitational radiation at a rate

$$\dot{M} \sim -GM^2R^4\omega^6 \sim -G\sigma M. \tag{23.1}$$

The lifetime of the piece is independent of its size,

$$\tau \sim M/|\dot{M}| \sim (G\sigma)^{-1}. \tag{23.2}$$

When the piece shrinks to a size smaller than μ/σ, its mass is determined mostly by the string, and the decay time is [see eq. (14.2)]

$$\tau \sim R/G\mu < (G\sigma)^{-1}. \tag{23.3}$$

The lifetime of the pieces can be smaller if they decay as a result of multiple self-intersections.

We see that, assuming a large intercommuting probability, the whole system decays no later than $\tau \sim (G\sigma)^{-1}$. The ratio of the mass density of walls and strings to the total density of the universe never exceeds

$$\left(\frac{\rho_{ws}}{\rho}\right)_{max} \sim \left(\frac{\tau}{\mu/\sigma}\right)^{1/2} G\mu \sim (G\mu)^{1/2}, \tag{23.4}$$

and thus the vacuum structures never dominate the universe.

The situation is changed if there is a period of inflation between the two phase transitions. Inflation can push the strings out to arbitrarily large scales; then the evolution of walls will proceed as discussed in section 21. It is conceivable that, after a "mild" inflation, the scale of strings is such that the walls are cut in pieces just when they are about to dominate the universe. The sizes of the pieces will then be comparable to their Schwarzschild radii, and a large number of black holes of mass $\sim(G^2\sigma)^{-1}$ can be formed. This sort of scenario has been discussed in ref. [64].

24. Monopoles connected by strings

Consider a model of the type (9.1), in which monopoles form at $T \sim \eta_m$ and then get connected by strings at $T \sim \eta_s < \eta_M$. One might expect the distribution of monopoles and antimonopoles at formation to be random, with usual $\sqrt{N}$ fluctuations of the magnetic charge:

$$\delta N \sim N^{1/2} \sim (L/\xi_M)^{3/2} . \tag{24.1}$$

Here, $N = N_+ + N_- \sim (L/\xi_M)^3$ is the total number of monopoles and antimonopoles in a volume L^3, $\delta N = N_+ - N_-$ is the magnetic charge fluctuation, and ξ_M is the correlation length. However, this expectation is wrong: positions of monopoles and antimonopoles at formation are strongly correlated [58]. To see this, note that the total magnetic charge inside a volume can be expressed as a surface integral over the boundary of the volume, where the integrand depends on the direction of the Higgs field at the boundary. For example, in the O(3) model of ref. [31]

$$\delta N = \frac{1}{8\pi} \oint |\phi|^{-3} \varepsilon_{abc} \phi^a \partial_i \phi^b \partial_j \phi^c \, dS^{ij} , \tag{24.2}$$

where ϕ^a is the Higgs field and dS^{ij} is the surface element. The integrand is $\sim \xi_M^{-1}$ and varies randomly on scales $\sim \xi_M$; hence

$$\delta N \sim L/\xi_M . \tag{24.3}$$

We see that δN goes like a square root of the surface area, not of the volume. In this sense the magnetic charge fluctuation (24.3) is just a surface effect, and there are no real volume charge fluctuations in the system [59].

Let us now turn to the second phase transition when the strings are formed. Assuming that no substantial monopole annihilation has occurred [10], the typical distance between the monopoles at that time is $d_0 \sim (\eta_M/\eta_s)\xi_M$. If both phase transitions are second-order, then $\xi_M \sim \eta_M^{-1}$, $\xi_s \sim \eta_s^{-1}$, and the string correlation length, ξ_s, is comparable to the average monopole separation, d_0. (If one or both transitions are first-order, ξ_s can be smaller or greater than d_0.) Most of the monopole–antimonopole pairs will be connected by the shortest possible strings of length $\sim d_0$. Some longer strings and closed loops should also be present, and the length distribution of strings can be found using a Monte Carlo simulation. A 3-dimensional simulation for this system is rather complicated and has not yet been done, while 2-dimensional simulations give [54, 60, 61]:

$$n_\ell \propto \exp(-\alpha \ell / d_0) , \tag{24.4}$$

where $\alpha \sim 1$ is a numerical factor. The exponential character of the distribution can be understood if we note that, as we go along a string, at each step there is a certain probability of getting the combination of phases corresponding to a monopole and terminating the string [62].

Even if the initial distribution of strings is not like (24.4), an exponential length distribution will be rapidly established as a result of intercommuting processes [7]. Long strings will be chopped into short pieces by intercommutings with much more numerous shorter strings (see fig. 9). The probability for a

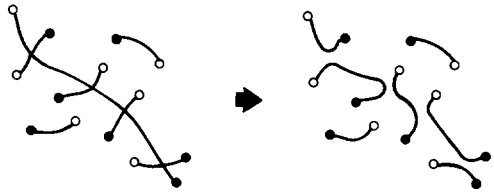

Fig. 9. Long strings are cut in small pieces by intercommuting with much more numerous shorter strings.

string of length ℓ to avoid intercommuting (per given time) is an exponentially decreasing function of ℓ, and thus strings much longer than d_0 will be exponentially suppressed.

The cosmological evolution of monopoles connected by strings has been discussed in refs. [7, 8]. When low-energy monopole and antimonopole get sufficiently close to one another, they rapidly annihilate [10]. The lifetime of a pair connected by a string is, therefore, determined by the time it takes to dissipate the energy of the string. The strings pull the monopoles with a force $f \sim \mu \sim \eta_s^2$, while the force of friction acting on a monopole is [see eq. (20.4)] $F_M \sim T^2 v$. At $T \ll \eta_s$, $F_s \ll f$ and friction is negligible. In general, monopoles have unconfined non-Abelian magnetic charges, and the dominant energy loss mechanism is the radiation of gauge quanta [7]. The classical dipole radiation formula gives

$$\dot{\varepsilon} \sim -g^{-2} W^2 \sim -(\mu/gm)^2 , \tag{24.5}$$

where g is the gauge coupling, $W = \mu/m$ is the monopole acceleration and $m \sim \eta_M/g$ is its mass. The lifetime of a pair connected by a string of length ℓ is

$$\tau \sim (\eta_M/\eta_s)^2 \ell . \tag{24.6}$$

It follows from (24.4) and (24.6) that the monopole density will decrease exponentially with time.

A somewhat different situation is obtained in Langacker–Pi-type models, where the string tension is $\mu \sim T^2$ (see section 9). In this case, we find from eq. (22.5) that the persistence length of strings at time t is

$$R(t) \sim (t_p/t)^{1/4}\, t \tag{24.7}$$

and never becomes comparable to the horizon size. Monopoles and antimonopoles are pulled together by the strings with a typical velocity v which can be found from $v^2 \sim (T^2/m)\, R(t)$. This gives

$$v(t) \sim (m_p/m)\, (t_p/t)^{1/4} . \tag{24.8}$$

[Equation (24.8) applies only for $t \gg (m_p/m)^4\, t_p$ when $v \ll 1$. At earlier times, the velocity of monopoles is determined by the balance of tension $\mu \sim T^2$ and friction $f \sim T^2 v$, which gives $v \sim 1$.] All $M\bar{M}$ pairs connected by strings much shorter than $v(t)\, t$ annihilate in less than one Hubble time.

If the strings disappear at temperature $T_f \ll T_s$, then assuming that monopole and string phase transitions are both second order and using eq. (24.4) we find that (for $T < T_f$)

$$\frac{n_M}{n_\gamma} \sim \exp\left\{-\alpha' \frac{m_p}{m} \left(\frac{T_s m_p}{T_f^2}\right)^{1/2}\right\} . \tag{24.9}$$

Here, n_M and n_γ are monopole and photon number densities, respectively, and α' is a numerical coefficient.

The evolution of monopoles connected by strings is different if there is a period of inflation between the two phase transitions (or if the monopole-forming phase transition is itself inflationary). In particular, if the monopoles are pushed beyond the present horizon, the evolution of strings is identical to that of topologically stable strings (section 22).

Finally, I should mention that some doubts have been raised about whether efficient monopole annihilation is consistent with causality. The argument is [63] that the magnetic charge fluctuations (24.3) cannot be erased on a timescale shorter than $t \sim L$. I think this argument is incorrect for several reasons. As explained above, there are no volume charge fluctuations in the system. The fluctuation (24.3) is just a surface effect which can be erased by a slight reshuffling of monopoles near the surface. But my main objection is given by the dynamical mechanism for monopole annihilation described above. As long as a physical mechanism does not require superluminal velocities, its efficiency is a dynamical question and is not constrained by any causality principles. For more discussion of this issue see refs. [59, 61, 63].

5. Cosmological effects of strings

25. Galaxy formation: Basic facts

Galaxies and clusters of galaxies have evolved by gravitational instability from small density fluctuations. The origin of the initial fluctuations is one of the major unresolved cosmological problems. Some density fluctuations can be produced at a phase transition in the early universe. However, it can be shown [11, 65] that physical processes at cosmic time t cannot produce substantial fluctuations on scales much greater than t. Phase transitions are expected to occur at $t < 10^{-4}$ s, and thus cannot explain density fluctuations on scales greater than a few parsec.

Two ways around this difficulty have been suggested. In inflationary scenario [23] all presently observable universe had initial size smaller than the horizon, and thus the horizon problem is avoided. Density fluctuations in this scenario are due to the quantum fluctuations of the Higgs field. An alternative possibility is that the density fluctuations are produced by strings [11, 12]. On scales greater than the horizon the density fluctuations due to strings are balanced by the corresponding variations in matter and radiation density. (On such scales the fluctuations are in the equation of state; density fluctuations of comparable magnitude can only be produced when the corresponding scale comes within the horizon [11, 65].) Rapidly moving open strings and oscillating closed loops produce density fluctuations on scales smaller than the horizon, so that the fluctuation-generating process continues for all times, extending to larger and larger scales. The string scenario of galaxy formation is discussed in the next section. Here we shall review some well-known results of the galaxy formation theory.

The evolution of density fluctuations is determined by two major effects: gravitational instability and dissipation. In discussing the gravitational aspects of the evolution, we shall use the following result of the linear perturbation theory [65].

Density fluctuation on a co-moving scale $\ell(t)$ grows like

$$\delta\rho/\rho \propto a(t) \propto (1+z)^{-1} \tag{25.1}$$

when $\ell(t)$ becomes greater than the Jeans length,

$$\lambda_J = (\pi v_s^2/G\rho)^{1/2} \sim 10 v_s t, \tag{25.2}$$

where v_s is the sound velocity. When $\ell(t) < \lambda_J$, $\delta\rho/\rho$ remains constant.

Comments: (i) This statement applies only to fluctuations on scales smaller than the horizon, but this is exactly the case we are interested in. (ii) In an open universe with $\Omega < 1$ the growth of density fluctuations stops at $z \sim \Omega^{-1}$. (iii) In a universe filled with two (or more) uncoupled components (say, radiation and axions), λ_J should be calculated for the component dominating the mass density*. (iv) Instead of the Jeans length λ_J it is often convenient to use the Jeans mass, which can be defined as the mass contained in a sphere of diameter λ_J:

$$M_J = (4\pi/3)\rho(\lambda_J/2)^3 . \tag{25.3}$$

During the radiation era, $t < t_{eq}$, the sound velocity is $v_s \sim 1$ and the Jeans length is $\lambda_J \sim t$. Hence, the density fluctuations produced by strings can start growing only at $t > t_{eq}$. The evolution at $t > t_{eq}$ is different for different types of dark matter dominating the universe, and we shall consider various cases separately.

(a) *Baryon-dominated universe.* Before decoupling, $t < t_{dec}$, baryons are coupled to radiation, so that $v_s \sim 1$ and $\lambda_J \sim t$. Thus, the density fluctuations start growing at $t \sim \max(t_{eq}, t_{dec})$. The discussion is simplified if we note that eqs. (2.17) and (2.18) require that $\Omega \sim 0.1$ in a baryon-dominated universe. For this value of Ω and $h \sim 1$, it follows from eqs. (2.22) and (2.24) that t_{eq} is not much different from t_{dec}, $t_{eq} \sim t_{dec}$. At $t \sim t_{dec}$ the sound velocity drops sharply from $v_s \sim 1$ to the thermal velocity of hot hydrogen gas, $v_s \sim 10^{-5}$, and the density fluctuations start growing on all scales of cosmological interest. An important dissipational effect in a baryon-dominated universe is the Silk damping: adiabatic density fluctuations are erased by photon viscosity on all mass scales smaller than

$$M_{silk} \sim 10^{12} (\Omega h^2)^{-2} M_\odot . \tag{25.4}$$

(b) *Neutrino-dominated universe* [66]. For simplicity we shall assume that only one of the 3 neutrino species has a Majorana mass $m_\nu \neq 0$. If the universe is dominated by these massive neutrinos, then

$$\Omega h^2 = 0.3 m_{30} \tag{25.5}$$

and $z_{eq} = 10^4 m_{30}$, where $m_{30} = m_\nu/30\,\text{eV}$. Neutrinos become nonrelativistic at $z \sim z_{eq}$, and for $z < z_{eq}$ their mean square velocity is

$$v = 6 \times 10^5 m_{30}^{-1}(1+z)\,\text{cm/s} . \tag{25.6}$$

The sound velocity is $v_s = 3^{-1/2} v$ and the Jeans mass is

$$\begin{aligned} M_J &= 1.3 \times 10^9 (1+z)^{3/2} m_{30}^{-7/2} M_\odot \\ &= M_{J,eq}[(1+z)/(1+z_{eq})]^{3/2} , \end{aligned} \tag{25.7}$$

* Independent fluctuations in the subdominant components can grow only logarithmically, and we shall disregard this effect here.

where $M_{J,eq} = 1.3 \times 10^{15}\, m_{30}^{-2}\, M_\odot \sim M_{eq}$. Here, M_{eq} is the mass within a sphere of diameter t at $t = t_{eq}$, $M_{eq} = 2 \times 10^{15}\, m_{30}^{-2}\, M_\odot$. In what follows we shall make no distinction between $M_{J,eq}$ and M_{eq}. Perturbations on mass scales $M < M_{eq}$ start growing at $z = z_M$, when the Jeans mass M_J drops down to M:

$$1 + z_M = (M/M_{eq})^{2/3}\,(1 + z_{eq})\,. \tag{25.8}$$

Neutrinos are non-interacting particles and erase their own density fluctuations on scales smaller than M_J by freely streaming out of overdensed regions. (For this reason, in scenarios with a primordial spectrum of adiabatic fluctuations, the density fluctuations survive only on scales greater than the maximum Jeans mass, $M_{J\,max} \sim M_{eq}$.)

(c) *Axion-dominated universe.* Axions are cold particles with thermal velocity very close to zero. They are not coupled to radiation, and perturbations in axions start growing at $t \sim t_{eq}$. There are no effective damping mechanism, and so the small-scale density fluctuations are not erased.

26. Strings and galaxy formation

In this section we shall find the spectra of density fluctuations generated by strings in various scenarios.

If one assumes that closed loops rapidly decay as a result of multiple intercommutings (which may be the case for global strings), then the density fluctuations produced on each scale at horizon crossing are of the order $(\delta\rho/\rho)_{hor} \sim \rho_{inf}/\rho$, where ρ_{inf} is the density due to infinite strings (see section 22). This gives [11]

$$(\delta\rho/\rho)_{hor} \sim A\, G\mu\,, \tag{26.1}$$

where $A \sim 30$ and $A \sim 6\pi$ for scales coming within the horizon at $t < t_{eq}$ and $t > t_{eq}$, respectively. This is the well-known scale-invariant (Zel'dovich) spectrum. The cosmological evolution of such a spectrum has been extensively discussed in the literature. Reasonable galaxy formation scenarios are obtained for $(\delta\rho/\rho)_{hor} \sim 10^{-4}$–$10^{-5}$. This corresponds to $G\mu \sim 10^{-6}$ and gives $\eta \sim 10^{16}$ GeV for local strings and $\eta \sim 10^{15}$ GeV for global strings. It is encouraging that the required value of η falls in the grand unification range.

A distinctive feature of the string scenario is the formation of planar wakes behind relativistically moving strings [20]. The wake formed behind a straight string has the shape of a wedge with an opening angle $\sim 8\pi G\mu$ (assuming that the velocity of the string is $v \sim 1$ and that the thermal velocity of the particles is smaller than $4\pi G\mu$). The wake formation is due to the conical nature of space around the string (see section 19) and in this sense is a purely kinematic effect. The density contrast in the wake is $\delta\rho/\rho \sim 1$, its length is $\sim t$ and its mass is comparable to that of the string: $M_w \sim 8\pi G\mu\, t^3\, \delta\rho \sim \mu\, t$. Particles enter the wake with a transverse velocity $v_t \sim 4\pi G\mu$. The gravitational acceleration in the field of the wake is $g \sim 2\pi G M_w/t^2$, and collisionless particles (like axions) do not escape much further than the width of the wake: $v_t^2/2g \sim 4\pi G\mu\, t$. Baryons will lose their transverse velocity in a shock and will stay confined within the width of the wake. Wakes formed behind rapidly moving strings can help to explain the observed large-scale structure in models with cold dark matter (axions).

We now turn to the scenario in which loops have long lifetimes,

$$\tau \sim R/\gamma G\mu\,, \tag{26.2}$$

where $\gamma \sim 100$ (see section 14). In this case galaxies and clusters condense around oscillating closed loops, while the loops gradually decay by gravitational radiation [12]. Although at present many properties of the loops can only be estimated in order-of-magnitude sense, it may be useful for future applications to be reasonably precise in normalization of certain quantities. We shall assume that the rate of loop formation is

$$\mathrm{d}n/\mathrm{d}t \sim \beta t^{-4} \tag{26.3}$$

[compare with (22.7)] and that the typical length of loops formed at time t is

$$R \sim \alpha t\,. \tag{26.4}$$

Note that here and below R stands for the *length* of the loops. Parameters α and β can be determined by a computer simulation of the evolution of strings. Here we shall assume that both α and β are not very different from 1.

Since the density fluctuations produced by strings cannot grow at $t < t_{\mathrm{eq}}$, one can start by calculating $\delta\rho/\rho$ at $t \sim t_{\mathrm{eq}}$. Like in section 22, we find the number density of loops at t_{eq}:

$$n_R(t_{\mathrm{eq}}) \sim \beta\alpha^{3/2}(R\,t_{\mathrm{eq}})^{-3/2}\,, \tag{26.5}$$

where

$$\gamma G\mu\, t_{\mathrm{eq}} \lesssim R \lesssim \alpha\, t_{\mathrm{eq}}\,. \tag{26.6}$$

Consider the density fluctuation on a scale $\ell < t_{\mathrm{eq}}$. A volume $\sim \ell^3$ will typically contain $N_R \sim n_R\ell^3$ loops of size R. The mass fluctuation induced by such loops is

$$\delta M \sim N_R^{1/2}\,\mu\, R \propto R^{1/4}\,. \tag{26.7}$$

This shows that the main contribution to δM is given by the largest loop in the volume, that is, by the loop of size R such that $N_R \sim 1$:

$$R \sim \alpha\beta^{2/3}\,\ell^2/t_{\mathrm{eq}}\,. \tag{26.8}$$

The corresponding density fluctuation is $\delta\rho \sim \mu R/\ell^3 \sim \alpha\beta^{2/3}\,\mu/\ell\, t_{\mathrm{eq}}$ and

$$(\delta\rho/\rho)_{\mathrm{eq}} \sim 30\,\alpha\beta^{2/3} G\mu\, t_{\mathrm{eq}}/\ell \sim 30\,\alpha\beta^{2/3}\, G\mu\,(M/M_{\mathrm{eq}})^{-1/3}\,. \tag{26.9}$$

Here, $M(M_{\mathrm{eq}})$ is the mass of matter within a sphere of diameter ℓ (t_{eq}). For 3 species of massless neutrinos ($N_\nu = 3$), $M_{\mathrm{eq}} = 5.5\times 10^{13}\,(\Omega h^2)^{-2}\,M_\odot$.

Equation (26.9) applies for $M_1 \lesssim M \lesssim M_2$, where

$$M_1 \sim \beta^{-1}(\gamma/\alpha)^{3/2}(G\mu)^{3/2}M_{\mathrm{eq}}\,, \qquad M_2 \sim \beta^{-1}M_{\mathrm{eq}}\,. \tag{26.10}$$

Loops on scales $M < M_1$ have decayed at $t < t_{eq}$, while loops on scale $M > M_2$ will form at $t > t_{eq}$. For $M < M_1$ density fluctuations do not grow between the loop decay and t_{eq}. Assuming that the fluctuations are not damped out, it is easily shown that on such scales

$$(\delta\rho/\rho)_{eq} \sim 30\,\alpha^{3/2}\,\beta\,\gamma^{-1/2}(G\mu)^{1/2}\,. \tag{26.11}$$

Fluctuations on scales $M > M_2$ are generated at $t_M \sim \frac{9}{2}\beta\,GM$. The magnitude of the fluctuations at that time is $\delta\rho/\rho \sim 6\,\pi\,\alpha\,\beta\,G\mu$. At later times $\delta\rho/\rho$ grows like $(1+z)^{-1}$ and we can write

$$\delta\rho/\rho \sim 6\,\pi\,\alpha\,\beta\,G\mu\,(t/t_M)^{2/3} \sim 6\,\pi\,\alpha\,\beta^{1/3}\,G\mu\,(M/M_{eq})^{-2/3}(1+z_{eq})/(1+z)\,. \tag{26.12}$$

The evolution of fluctuations for $M < M_2$ is different for different types of dark matter dominating the universe, and we shall consider various cases separately [13].

(a) *Baryon-dominated universe.* Density fluctuations produced by the loops which decayed before $t_{dec} \sim t_{eq}$ are erased by Silk damping. At $t \sim t_{dec} \sim t_{eq}$ baryons pick up the fluctuations produced by surviving loops, and at later times

$$\delta\rho/\rho \sim (\delta\rho/\rho)_{eq}(1+z_{eq})/(1+z) \tag{26.13}$$

for $M_1 < M < M_2$.

Statistical analysis of galaxy distribution suggests [65] that the maximum scale that has gone nonlinear at present is $\sim 8\,h^{-1}\,M_{pc}$, which corresponds to $M_{n\ell} \sim 6\times 10^{14}\,\Omega\,h^{-1}\,M_\odot$. To normalize the spectrum of fluctuations, we shall require that $\delta\rho/\rho \sim 1$ for $M \sim M_{n\ell}$ at $z \sim \Omega^{-1}$. ($\Omega \sim 0.1$ in a baryon-dominated universe.) This determines the value of $G\mu$:

$$G\mu \sim 4\times 10^{-6}\,\alpha^{-1}\,\beta^{-2/3}(\Omega\,h)^{-1}\,. \tag{26.14}$$

The resulting spectrum of fluctuations is shown in fig. 10 for $\Omega \sim 0.1$, $\alpha \sim \beta \sim h \sim 1$ and $\gamma \sim 100$. This spectrum corresponds to the gravitational clustering picture: the fluctuations increase towards smaller scales*. The lower cut-off of the spectrum is at $M_1 \sim 10^{12}\,M_\odot$. It gives the mass of the first objects to be

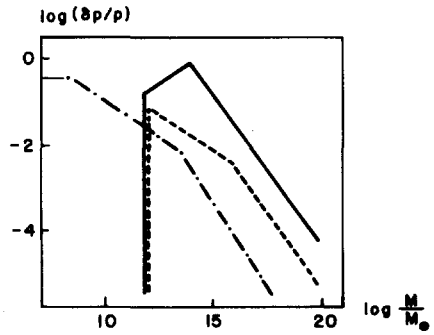

Fig. 10. The spectrum of density fluctuations in (solid curve) neutrino-, (dashed curve) baryon-, and (dashed-dotted curve) axion-dominated universe. The scale of $\delta\rho/\rho$ is arbitrary.

* An abrupt change of slope of $\delta\rho/\rho$ at $M = M_1$, M_2 is, of course, an artifact of our approximations. A more accurate analysis should give smooth transitions between different regimes.

formed. Interestingly enough, M_1 is the typical mass of a large galaxy. In this scenario galaxies start forming at $z \sim 40$.

(b) *Neutrino-dominated universe.* Neutrinos erase their density fluctuations on scales smaller than their Jeans mass, $M < M_J$, but when M_J drops down to M, they pick up the fluctuations produced by surviving loops. Hence, we can write

$$\delta\rho/\rho \sim (\delta\rho/\rho)_{eq}(1+z_M)/(1+z) \propto M^{1/3}, \tag{26.15}$$

where z_M is given by eq. (25.8). Equation (26.15) applies for $M_\nu < M < M_2$, where

$$M_\nu \sim \alpha^{-3/5}\beta^{-2/5}(\gamma G\mu)^{3/5} M_{eq}. \tag{26.16}$$

Loops on scales $M < M_\nu$ decay at $z > z_M$. For $M > M_2$ the spectrum is given by eq. (26.12).

The spectrum we have obtained has a maximum at $M \sim M_2$, which is the first scale to go nonlinear in this model. Requiring that at present $\delta\rho/\rho \sim 1$ for $M \sim M_{n\ell}$, we obtain

$$G\mu \sim 4\times 10^{-6}\alpha^{-1}\beta^{-1/3}. \tag{26.17}$$

Figure 10 shows the spectrum of density fluctuations for $\Omega \sim h \sim \alpha \sim \beta \sim 1$ and $\gamma \sim 100$. In this case $m_\nu \sim 100$ eV, $M_2 \sim M_{eq} \sim 10^{14} M_\odot$ and $M_\nu \sim 10^{12} M_\odot$. Pancakes of mass $\sim M_{eq}$ collapse at $z \sim 1$. In our model (unlike the standard pancake scenario) the pancake fragmentation is helped along by the presence of perturbations on scales $M_\nu < M < M_{eq}$. Note that M_ν has the order-of-magnitude of a typical galactic mass.

(c) *Axion-dominated universe.* In the axion-dominated case perturbations on all scales start growing at $t \sim t_{eq}$. There are no efficient damping mechanisms, and the fluctuations on scales $M < M_2$ are given by eq. (26.13), where $(\delta\rho/\rho)_{eq}$ is given by (26.9) and (26.11) for $M > M_1$ and $M < M_1$ respectively. Figure 10 shows the spectrum of fluctuations for $\Omega \sim h \sim \alpha \sim \beta \sim 1$ and $\gamma \sim 100$. Like in the baryon-dominated case, this spectrum corresponds to the gravitational clustering picture. Baryons pick up the axion density fluctuations at $t > t_{dec}$.

The analysis of this section shows that strings of a typical grand unification mass scale can lead to reasonable scenarios for galaxy formation in a universe dominated either by baryons, neutrinos or axions. In fact, the string model has some advantages in all three cases, compared to the standard scenario with adiabatic fluctuations. A detailed discussion of galaxy formation scenarios is beyond the scope of this review, and I will only mention the relevant points.

(i) Density fluctuations produced by strings are not in the form of waves with random phases; this can explain the observed deviations from the Gaussian behavior. For example, rare supergiant loops can produce localized regions of density contrast much greater than one would expect from Gaussian fluctuations [20]. Occasional splitting of loops can help to explain the observed cluster–cluster correlations [67].

(ii) Closed loops have sizes much smaller than those of the galaxies condensing around them. A loop representing a small density fluctuation on the galactic scale produces a large density contrast in its immediate vicinity. This results in accretion of matter onto the loops and formation of massive compact objects, which can be identified with quasars and active galactic nuclei [20, 21]. Early formation of quasars can reionize the universe, smoothing out small-scale temperature fluctuations, and thus resolve one of the difficulties of the baryon-dominated scenario. It can also explain the existence of quasars at $z \sim 1$ in neutrino-dominated model, which requires the pancake collapse at $z < 0.5$.

(iii) The galactic mass $\sim 10^{12} M_\odot$ naturally arises as a cut-off of the spectrum in baryon- and neutrino-dominated cases.

(iv) Finally, wakes formed behind long, rapidly moving strings can help to explain the observed large-scale structure in the axion-dominated case.

It should be noted that the string scenario of galaxy formation assumes that the universe is initially homogeneous and isotropic on scales much greater than the horizon. Such initial conditions can be explained if we assume that there was a period of inflation before the string formation. An example of a grand unified model which gives both a satisfactory inflationary scenario and strings of required energy scale is given in ref. [30].

27. *Observational effects of strings*

If strings indeed cause the galaxy formation, they should also produce a number of unique observational side effects. Some of these effects will soon be within the experimental limits, which will allow to rule out or confirm the string scenario. Even if strings have nothing to do with galaxies, their detection would, of course, be extremely interesting. However, it appears that strings with $G\mu \ll 10^{-6}$ will be very difficult to observe. In this section I shall briefly discuss various observational effects of strings. For more details the reader is referred to the original literature.

Gravitational waves emitted by oscillating loops add up to a stochastic gravitational wave background. Loops of size R radiate at frequencies $\omega \sim R^{-1}$; after the waves are emitted, their frequency is red shifted like $\omega \propto (1+z)$. Presently surviving loops have extremely low frequencies, and the flux they produce is well below the observational capabilities [39, 68]. With $G\mu \sim 10^{-6}$, waves which now have periods less than 10^3 years correspond to loops that formed and decayed during the radiation era.

A convenient measure of the intensity of the radiation is

$$\Omega_g(\omega) = \frac{\omega}{\rho_c}\frac{d\rho_g}{d\omega}. \tag{27.1}$$

Here ρ_g is the energy density of the gravitational waves and ρ_c is the critical density. $\Omega_g(\omega)$ gives the energy density in units of ρ_c per logarithmic frequency interval.

Loops decaying at time $\sim t$ during the radiation era ($t < t_{eq}$) have size $R \sim \gamma G\mu t$ and produce gravitational waves of frequency $\sim R^{-1}$ and energy density

$$\rho_g \sim \mu R n_R \sim \alpha^{3/2}\beta\gamma^{-1/2}(G\mu)^{1/2}(Gt^2)^{-1}, \tag{27.2}$$

where α and β are the parameters introduced in the previous section. Since ρ_g redshifts in the same way as the radiation density ρ_γ, we can write [18]*

$$\Omega_g(\omega) \sim 30\,\alpha^{3/2}\beta\gamma^{-1/2}(G\mu)^{1/2}\Omega_\gamma, \tag{27.3}$$

where $\Omega_\gamma = \rho_\gamma/\rho_c = 2\times 10^{-5}h^{-2}$. With $G\mu \sim 10^{-6}$, $\alpha \sim \beta \sim 1$ and $\gamma \sim 100$ this gives

* Two effects not taken into account in eq. (27.3) are: (i) radiation of a single loop is spread over a range of frequencies (see section 14) and (ii) as the loop decays, its frequency gradually changes. A more careful estimation [41] does not change the order of magnitude in (27.3).

$$\Omega_g(\omega) \sim 10^{-7} h^{-2}. \tag{27.4}$$

This equation applies for waves with present frequencies $\omega \geq (1+z_{eq})^{-1}$, $(\gamma G\mu\, t_{eq})^{-1} \sim 4\times 10^{-4}\,\Omega h^2\,\mathrm{yrs}^{-1}$. The spectrum at smaller frequencies is discussed in refs. [18, 19].

Recent observations of the millisecond pulsar imply [19] that $\Omega_g < 10^{-5}$ for gravitational waves with periods $\sim$1 year. However, the accuracy grows rapidly with the time of observation, and $\Omega_g \sim 10^{-7}$ will probably become detectable within several years.

If the loops rapidly deteriorate because of self-intercommutings, the energy density of gravitational waves is very small (Ω_g is proportional to $(G\mu)^2$ [18]). In this case most of the loop energy goes into ultrarelativistic particles. The typical energy of the decay products is

$$\varepsilon \sim \eta(1-f)^{-n}, \tag{27.5}$$

where n is given by eq. (13.3) and f is the fraction of loop energy that goes into kinetic energy of daughter loops. For the sake of illustration take $f = 0.5$. (With this choice the equations considerably simplify, but this value of f is probably too large.) Then the loops decaying at time t produce particles of energy

$$\varepsilon \sim \eta(\eta\, t)^{1/2} \sim m_p (G\mu)^{3/4} (t/t_p)^{1/2}, \tag{27.6}$$

where $t_p \sim 10^{-43}$ s is the Planck time and $m_p \sim 10^{19}$ GeV is the Planck mass. With $G\mu \sim 10^{-6}$, particles being produced at present have energies $\sim 10^{44}$ GeV! Nongravitational interactions of such particles are extremely weak. The cross-section for scattering on photons of the microwave background is $\sigma \sim \alpha_G^2 \varepsilon_{cm}^{-2} \sim \alpha_G^2/\varepsilon T$, where $\varepsilon_{cm} \sim (\varepsilon T)^{1/2}$ is the center-of-mass energy, T is the temperature and α_G is the gauge coupling squared. The typical interaction time is

$$\tau_\gamma \sim (n_\gamma \sigma)^{-1} \sim \varepsilon/\alpha_G^2 T^2 \sim \Omega_\gamma^{-1/2} (\varepsilon/m_p) t \gg t, \tag{27.7}$$

where $n_\gamma \sim T^3$ is the photon number density. The gravitational interaction cross-section is $\sigma_g \sim (G\varepsilon_{cm})^2 \sim \varepsilon\, T/m_p^4$ and the interaction time is $\tau_g \sim \Omega_\gamma^{-1}(m_p/\varepsilon)(t/t_p)t \gg t$. Eventually the particles are slowed down by expansion to energies $\ll m_p$. Then τ_γ becomes less than the Hubble time, the particles lose the remaining energy by pair production, and the pairs lose most of their energy by inverse Compton scattering [19]. Pairs being produced today are due to the loops that decayed at $t \sim 10^{-10}$ s. The resulting γ-ray spectrum peaks at $m_e^2/T \sim 10^5$ GeV. However, the initial energy of the loops is red shifted by a factor $\sim \Omega_\gamma$ compared to that of matter, and so

$$\Omega_{\gamma\mathrm{ray}} \sim 30 G\mu\, \Omega_\gamma \sim 10^{-9}. \tag{27.8}$$

This value is consistent with observational constraints, $\Omega_{\gamma\mathrm{ray}} < 10^{-7}$. (Here I disagree with the conclusion of ref. [19], where the redshift effect is not taken into account.) Note that, although most of the numerical values in this discussion are very sensitive to the assumed value of f, the estimate (27.8) is not.

Another observational prediction of the string scenario is the formation of double images of objects located behind the strings [14]. The typical separation between the images is

$$\delta \sim 4\pi G\mu \tag{27.9}$$

(see section 19). With $G\mu \sim 10^{-6}$–10^{-5} this gives $\delta \sim 3$–30 arc sec. The probability for a quasar to be lensed by a string is [15] $\sim \frac{1}{2}\alpha\beta\delta \ln(\gamma\delta)^{-1}$. With $\sim 10^4$ known quasars, the expected number of double quasars is ~ 1. It is not excluded that some of the known double quasars are due to strings [15–17]. Galaxies are much more numerous than quasars, and one can search for lines of double galaxies along open strings or large closed loops [15, 16].

Kaiser and Stebbins [22] have pointed out that strings should leave a characteristic signature on the microwave background: the background temperature should have steplike discontinuities on curves on the sky. This effect is similar to the wake formation behind a moving string. The co-moving frames on different sides of the wake move towards each other with a velocity $\sim 8\pi G\mu v$, where v is the transverse velocity of the string. As a result, the observer will find the radiation on the trailing side of the string blue shifted compared to that on the leading side. With $v \sim 1$ the corresponding temperature fluctuation is $\delta T/T \sim 8\pi G\mu v \sim 10 G\mu$. Present observational limits are consistent with $G\mu \lesssim 10^{-5}$.

28. String-dominated universe

As we discussed in section 22, noncommuting strings with non-Abelian $\pi_1(M)$ and Z_n strings with $n \geq 3$ can form stable networks and eventually dominate the universe. In this section we shall consider the possibility that our universe is in fact string-dominated [69].

Suppose the strings are formed at $t \sim t_0$ and that the correlation length at the phase transition is $\xi < t_0$. The energy density of strings at that time is $\rho_s(t_0) \sim \mu\xi^{-2}$. At later times the strings are just stretched by the expansion of the universe, $\rho_s(t) \propto a^{-2}(t)$. The time t_s when the universe becomes string-dominated can be found from (assuming $t_s > t_{eq}$)

$$\rho_s/\rho(t_s) \sim G\mu(t_0/\xi)^2(t_{eq}/t_0)(t_s/t_{eq})^{2/3} \sim 1 . \tag{28.1}$$

For $t > t_s$, using the evolution equation $(\dot{a}/a)^2 \sim G\rho_s \propto a^{-2}$, we find that the universe expands like

$$a(t) \propto t . \tag{28.2}$$

This is the same t-dependence as one finds in a universe with $\Omega < 1$ at redshifts $2 + z \ll \Omega^{-1}$ [65]. Thus, a universe with $\Omega = 1$ which becomes string-dominated at a redshift z_s mimics the behavior of a universe with $\Omega \sim (2 + z_s)^{-1} < 1$.

The value of Ω very close to 1 is predicted by the inflationary scenario [23]. On the other hand, there is strong observational evidence indicating that $0.2 \lesssim \Omega \lesssim 0.5$. This discrepancy can be resolved if the universe becomes dominated by strings at $0 \lesssim z_s \lesssim 3$.

Requiring that $t_s \sim 10^{17}$ s and using the values $t_{eq} \sim 10^{11}$ s, $t_0 \sim m_p/\eta^2$ [see eq. (2.9)], we find from eq. (28.1)

$$\eta \sim 10^4(\xi/t_0)^{1/2}\,\text{GeV} \lesssim 10^4\,\text{GeV} . \tag{28.3}$$

The corresponding value of $G\mu$ is $\lesssim 10^{-30}$. The typical distance between the strings is $\sim (G\mu)^{1/2} t_{pres} \lesssim 10^{13}$ cm, where $t_{pres} \sim 10^4$ Mpc is the present cosmic time. Although the nearest string may be closer to us than the Sun, its experimental detection seems nearly impossible. Local gravitational effects of strings with $G\mu \lesssim 10^{-30}$ are totally negligible, and even if the observer is so lucky that the string passes through his own body, he will hardly notice it.

It should be noted that no realistic grand unified models have been suggested which predict strings developing stable networks at such a low-energy scale ($\eta \lesssim 10^4$ GeV). The universe can also be dominated by "regular" strings, which are still moving at relativistic speeds, but have vanishingly small intercommuting probability. The condition for η in this case is [69] $\eta \lesssim 10^9$ GeV.

Acknowledgements

I would like to thank A.E. Everett, C.J. Hogan, T.W.B. Kibble, G. Lazarides, M. Rees, Q. Shafi, P. Shellard, N. Turok and T. Vachaspati for discussions.

References

[1] D.A. Kirzhnits, JETP Lett. 15 (1972) 745.
[2] A.D. Linde, Rep. Prog. Phys. 42 (1979) 389;
S. Weinberg, Phys. Rev. D9 (1974) 3357;
L. Dolan and R. Jackiw, Phys. Rev. D9 (1974) 3320.
[3] T.W.B. Kibble, J. Phys. A9 (1976) 1387; Phys. Reports 67 (1980) 183; in: Quantum structure of space-time, eds. M.J. Duff and C.J. Isham (Cambridge University Press, Cambridge, 1982).
[4] T.W.B. Kibble, G. Lazarides and Q. Shafi, Phys. Rev. D26 (1982) 435.
[5] A. Vilenkin and A.E. Everett, Phys. Rev. Lett. 48 (1982) 1867.
[6] A.E. Everett and A. Vilenkin, Nucl. Phys. B207 (1982) 43.
[7] A. Vilenkin, Nucl. Phys. B196 (1982) 240.
[8] G. Lazarides, Q. Shafi and T. Walsh, Nucl. Phys. B195 (1982) 157.
[9] Ya. B. Zel'dovich, I. Yu. Kobzarev and L.B. Okun, Zh. Eksp. Teor. Fiz. 67 (1974) 3 [Sov. Phys. JETP 40 (1975) 1].
[10] J.P. Preskill, Phys. Rev. Lett. 43 (1979) 1365.
[11] Ya. B. Zel'dovich, Mon. Not. R. Astr. Soc. 192 (1980) 663.
[12] A. Vilenkin, Phys. Rev. Lett. 46 (1981) 1169, 1496 (E).
[13] A. Vilenkin and Q. Shafi, Phys. Rev. Lett. 51 (1983) 1716.
[14] A. Vilenkin, Phys. Rev. D23 (1981) 852.
[15] A. Vilenkin, Ap. J. Lett. 282 (1984) L51.
[16] J.R. Gott, Ap. J. 288 (1985) 422.
[17] C.J. Hogan and R. Narayan, M.N.R.A.S. 211 (1984) 575.
[18] A. Vilenkin, Phys. Lett. 107B (1981) 47.
[19] C.J. Hogan and M.J. Rees, Nature 311 (1984) 109.
[20] J. Silk and A. Vilenkin, Phys. Rev. Lett. 53 (1984) 1700.
[21] C.J. Hogan, Phys. Lett. 143B (1984) 87.
[22] N. Kaiser and A. Stebbins, Nature 310 (1984) 391.
[23] The Very Early Universe, eds. G.W. Gibbons, S.W. Hawking and S.T.C. Siklos (Cambridge University Press, Cambridge, 1983).
[24] P.J.E. Peebles, Physical Cosmology (Princeton University Press, Princeton, 1971).
[25] S. Coleman, in: New Phenomena in Subnuclear Physics, ed. A. Zichichi (Plenum, NY, 1977).
[26] H.B. Nielsen and P. Olesen, Nucl. Phys. B61 (1973) 45.
[27] T.W.B. Kibble, G. Lazarides and Q. Shafi, Phys. Lett. 113B (1982) 237.
[28] D. Olive and N. Turok, Phys. Lett. 117B (1982) 193.
[29] G. Toulouse, J. Physique Lett. 38 (1976) L-67.
[30] Q. Shafi and A. Vilenkin, Phys. Rev. D29 (1984) 1870.
[31] G. t'Hooft, Nucl. Phys. B79 (1974) 276;
A.M. Polyakov, JETP Lett. 20 (1974) 194.
[32] P. Langacker and S.-Y. Pi, Phys. Rev. Lett. 45 (1980) 1.
[33] R. Peccei and M.R. Quinn, Phys. Rev. Lett. 38 (1977) 1440;
M. Dine, W. Fischler and M. Srednicky, Phys. Lett. 104B (1981) 199.
[34] P. Sikivie, Phys. Rev. Lett. 48 (1982) 1156.
[35] G. Lazarides and Q. Shafi, Phys. Lett. 115B (1982) 21.

[36] P. Goddard, J. Goldstone, C. Rebbi and C.B. Thorn, Nucl. Phys. B56 (1973) 109.
[37] J. Scherk, Rev. Mod. Phys. 47 (1975) 123.
[38] A. Vilenkin, Phys. Rev. D24 (1981) 2082.
[39] N. Turok, Nucl. Phys. B242 (1984) 520.
[40] T.W.B. Kibble and N. Turok, Phys. Lett. 116B (1982) 141.
[41] T. Vachaspati and A. Vilenkin, Phys. Rev. D., in press.
[42] P. Shellard, private communication.
[43] S. Weinberg, Gravitation and Cosmology (Wiley, New York, 1972).
[44] T. Vachaspati, A.E. Everett and A. Vilenkin, Phys. Rev. D, in press.
[45] N. Turok and P. Bhattacharjee, Phys. Rev. D.
[46] A. Albrecht and N. Turok, private communication.
[47] A. Vilenkin (unpublished).
[48] L.H. Ford and A. Vilenkin, J. Phys. A14 (1981) 2353.
[49] A. Vilenkin, Phys. Lett. 133B (1983) 177.
[50] J. Ipser and P. Sikivie, Phys. Rev. D30 (1984) 712.
[51] A.E. Everett, Phys. Rev. D10 (1974) 3161.
[52] A.E. Everett, Phys. Rev. D24 (1981) 858.
[53] J.A. Harvey, E.W. Kolb, D.B. Reiss and S. Wolfram, Nucl. Phys. B201 (1982) 16.
[54] T. Vachaspati and A. Vilenkin, Phys. Rev. D30 (1984) 2036.
[55] D. Stauffer, Phys. Reports 54 (1979) 1.
[56] T.W.B. Kibble, Nucl. Phys., in press.
[57] A. Vilenkin, in: Inner Space/Outer Space (Chicago University Press, Chicago, 1984).
[58] M.B. Einhorn, D.L. Stein and D. Toussaint, Phys. Rev. D21 (1980) 3295.
[59] A. Vilenkin, Phys. Lett. 136B (1984) 47.
[60] P. Sikivie, Proc. Summer School on Particle Physics, Gif-sur-Yvette, 1983.
[61] A.E. Everett, T. Vachaspati and A. Vilenkin, Phys. Rev. D, in press.
[62] P. Sikivie, private communication.
[63] E. Weinberg, Phys. Lett. 126B (1983) 441.
[64] F. Stecker and Q. Safi, Phys. Rev. Lett. 50 (1983) 928.
[65] P.J.E. Peebles, The Large Scale Structure of the Universe (Princeton University Press, Princeton, 1980).
[66] J.R. Bond, G. Efstathiou and J. Silk, Phys. Rev. Lett. 45 (1980) 1980.
[67] N. Turok and D.N. Schramm, Nature 312 (1984) 598;
J. Preskill and M. Wise, unpublished.
[68] E. Witten, Phys. Rev. D30 (1984) 272.
[69] A. Vilenkin, Phys. Rev. Lett. 53 (1984) 1016.

Note added in proof

I would like to mention some interesting new developments that occurred after this paper was submitted.

(1) Albrecht and Turok [70] have done a direct numerical simulation of the evolution of strings. They used the method of ref. [54] to simulate the phase transition and evolved the resulting system of strings by solving numerically the dynamical equations of motion. The intercommuting probability for intersecting strings was assumed equal to one. The results of the simulation are basically in agreement with the scenario of string evolution described in section 22 and, in fact, put that scenario on a firmer basis.

(2) Witten has shown [71] that in some grand unified models electromagnetic gauge invariance can be spontaneously broken inside the strings. Such strings would behave as superconducting wires. If an electric field E is applied along a superconducting string, the current builds up at the rate $\mathrm{d}i/\mathrm{d}t = \beta(ce^2/\hbar)E$, where e is the gauge coupling and β is a model-dependent numerical coefficient. When the current reaches a critical value $i_{\max}$, its growth terminates and the string starts producing particles at the rate $\mathrm{d}^2N/\mathrm{d}t\,\mathrm{d}\ell \sim (e/\hbar)E$. The magnitude of $i_{\max}$ is also model-dependent, but does not exceed $e\eta/\hbar$, where η is the energy scale of the string.

Before Witten's paper it appeared that strings can manifest themselves only through their gravitational

interactions. However, superconducting strings can have very interesting interactions with cosmic magnetic fields. Consider a string moving through a magnetized plasma with a velocity $\boldsymbol{v}$. In the frame of the string there is an electric field $\boldsymbol{E} = c^{-1}\boldsymbol{v} \times \boldsymbol{B}$, and the current builds up at the rate $\mathrm{d}i/\mathrm{d}t \sim (e^2/\hbar)vB$. This current creates its own magnetic field which in turn acts on the plasma. The physics of these interactions of strings with cosmic plasmas is not well understood. Some interesting possibilities are indicated in refs. [71, 72].

[70] A. Albrecht and N. Turol, Phys. Rev. Lett., in press.
[71] E. Witten, Princeton University Preprint (1984).
[72] A. Vilenkin, in: Proc. 12th Texas Symp. on Relativistic Astrophysics (Jerusalem, 1984).